Egyptian Journal of Aquatic Biology & Fisheries
Zoology Department, Faculty of Science,
Ain Shams University, Cairo, Egypt.
ISSN 1110 – 6131
Vol. 26(4): 905 – 936 (2022)
www.ejabf.journals.ekb.eg

Evaluation of Contamination Status, Ecological and Human Health Risks of Heavy Metals in Sediments North of Safaga Bay along the Red Sea, Egypt

Aida H. Shobier*, Ghada F. El-Said, Mona Kh. Khalil,
Mohamed Abd El Wahab, and Mahmoud I. I. Mohamaden
National Institute of Oceanography and Fisheries, NIOF, Cairo, Egypt.

***Corresponding Author: aida_shobier@hotmail.com**

ARTICLE INFO

Article History:
Received: July 13, 2022
Accepted: July 26, 2022
Online: Aug. 19, 2022

Keywords:
Heavy metals,
Sediment quality,
Environmental risk,
Human health risk,
Safaga Bay

ABSTRACT

This study aimed to estimate the contamination levels and potential risks of some heavy metals (Al, Fe, Mn, Zn, Cu, Co, Ni, Pb, and Cd) in surface sediments collected from northern Safaga Bay along the Egyptian Red Sea coast. The concentrations of the studied metals decreased in the following order: Al> Fe> Mn> Zn> Pb> Ni> Co> Cu> Cd, with average concentrations of 4537.12±5025.35 mg/kg dw, 678.91±342.97 mg/kg dw, 136.09±117.00 mg/kg dw, 40.38±11.92 mg/kg dw, 17.19±3.97 mg/kg dw, 12.74±3.01 mg/kg dw, 9.24±2.19 mg/kg dw, 2.98±1.24 mg/kg dw, and 2.46±1.20 mg/kg dw, respectively. Results of sediment contamination indices such as contamination factor (*CF*), degree of contamination (C_d), modified degree of contamination (mC_d), metal pollution index (*MPI*), enrichment factor (*EF*), potential contamination index (PCI_i), sediment pollution index (*SPI*), and potential ecological risk index (*RI*) showed that the sampling sites are rated between uncontaminated and highly polluted. According to sediment quality guidelines (*SQGs*), adverse biological effects of heavy metals have sometimes been associated with Cd, and more rarely with Zn, Cu, Ni and Pb. Interestingly, sediment quality indices indicated the critical hazards of Cd to the biological system in the study area. The results of the assessment of risks to human health by heavy metals in sediments demonstrated that their exposure did not pose any carcinogenic risks. Statistical analyses revealed the interaction between geochemical variables, the distribution of heavy metals**,** as well as the proximity to pollution sources and flowing water.

INTRODUCTION

The coastal environment is increasingly affected by heavy metal pollutants due to the development of global industry. Heavy metals pollution is one of the most harmful threats to natural marine ecosystems **(Vasiliu *et al.*, 2020; Khaled *et al.*, 2021)**. Heavy metals are toxic pollutants that have serious effects on the environment, non-biodegradable, biomagnify and accumulate in the food chain **(Maanan *et al.*, 2014; Billah *et al.*, 2017; Khaled *et al.*, 2021)**.

Since heavy metals exist in both solid and dissolved forms, they have a significant impact on many geochemical and biological cycles. Marine sediments are reservoirs of heavy metals and other hazardous pollutants along with terrestrial particles and shell debris **(Wang *et al.*, 2020)**. They can be used to determine the

source of toxic substances, identify pathways for diffusion, and identify drains of pollutants in aquatic systems **(Vasiliu *et al.*, 2020)**.

In the last decade, numerous studies have been conducted on metal pollution in coastal areas and its ecological impact on natural ecosystems **(Ayadi *et al.*, 2015; Islam *et al.*, 2015; Wang *et al.*, 2015a, b; El Nemr *et al.*, 2016a, b)**. These studies aimed to assess the impact of human performance on marine ecosystems and sediment quality that reflects the pollution status of the ecosystem **(Khaled *et al.*, 2021)**.

The Red Sea is a semi-enclosed sea, famous for its clear and warm waters **(Gladstone *et al.*, 2013)**. It extends between latitudes 22.25^{o} and 27.25^{o} N and longitudes 33.83^{o} and 37.83^{o} E. It contains extensive coral reefs, mangroves and seagrass habitats and supports a high degree of diversity **(Pan *et al.*, 2011)**.

The Red Sea is used as a meeting point and a place of transportation from the Mediterranean Sea and the Indian Ocean, and is therefore susceptible to pollution from major metals and oil **(Badawy *et al.*, 2018)**. Besides oil spills affecting the Red Sea, there are also many sources of pollution such as wastewater discharge, fishing, shipping, oil drilling, aquaculture, desalination discharges, construction activities along the seashore, terrestrial runoff, plastic waste, maritime traffic, and phosphate shipping pollution activities **(El-Sikaily *et al.*, 2005; El Nemr *et al.*, 2016a, b)**.

These activities pollute the surrounding area with heavy metals and organic compounds as well; e.g. PAHs **(Ugochukwu & Leton, 2004; Fiedler *et al.*, 2009)**. Several studies have been conducted on the sediments of the Red Sea in Egypt **(Badawy *et al.*, 2018; El-Taher *et al.*, 2018; Nour *et al.*, 2018; Carvalho *et al.*, 2019; Ibrahim *et al.*, 2019; El-Sikaily *et al.*, 2021; Nour *et al.*, 2022; Soliman *et al.*, 2022)**.

This research aimed to: (1) study the spatial variation of some physical and chemical variables in seawater and sediments in relation to the content of heavy metals in the sediments of North Safaga area, (2) estimate the anthropogenic participation of heavy metal content in the study area using some ecological risk indices, (3) demonstrate the potential link between heavy metals contamination of sediments and adverse biological effects on aquatic organisms based on the widely accepted sediment quality guidelines and statistical analyses, and (4) assess the risks of ingestion, dermal contact and swimming ingestion of heavy metals in sediments to human health.

MATERIALS AND METHODS

Sampling Area

Safaga Bay is a shallow bay with a maximum depth of 70 m and is located on the western side of the Red Sea. The bay is bounded on the west by a narrow dry coastal plain, while the eastern and southern regions are bordered by steep cliffs. The northern border is bounded by the well-known Ras Abu Soma Peninsula **(Abd El Wahab *et al.*, 2011)**. The water current of the bay moves from the North side to the South side. Therefore, the bay is divided into the North Safaga and South Safaga. The studied region extends from latitudes 26.75° to 26.78° N and longitudes 33.95° to 33.97° E (Fig. 1). This region represents three different environmental characteristics, including the tidal zone, the reef zone and the marine zone. The lower northern part of Safaga Bay contains coral reef and seagrass communities. The distinctive southern part of Safaga Bay is affected by the effects of the activities of Safaga Port and the Abu Tartour phosphate project **(Abd El Wahab *et al.*, 2011)**. Additionally, this

region plays an important role in the international trade of Egypt, characterized by a large volume of transport and frequent loading and unloading. The port includes passenger and shipping terminals for bauxite, coal, grain, quartz and orthoclase **(Mansour *et al.*, 2013; El-Metwally *et al.*, 2017)**.

Sampling

Thirteen samples of surface sediments were collected during 2017 from different stations in Safaga Bay along the Red Sea coast using a grab sampler (Table 1 & Fig. 1). During the sampling process, physical parameters such as seawater temperature (T, ºC), salinity (S‰), pH, dissolved oxygen (DO, mg/L) and electrical conductivity (EC, mS/cm) were measured on site with a Hanna instrument (Ha 9828). Positions were recorded by two Global Position System GPS (Magellan, 1000, 5000 pro) and the depth was measured by an echo sounder (ONWA-KF-667-dual frequency).

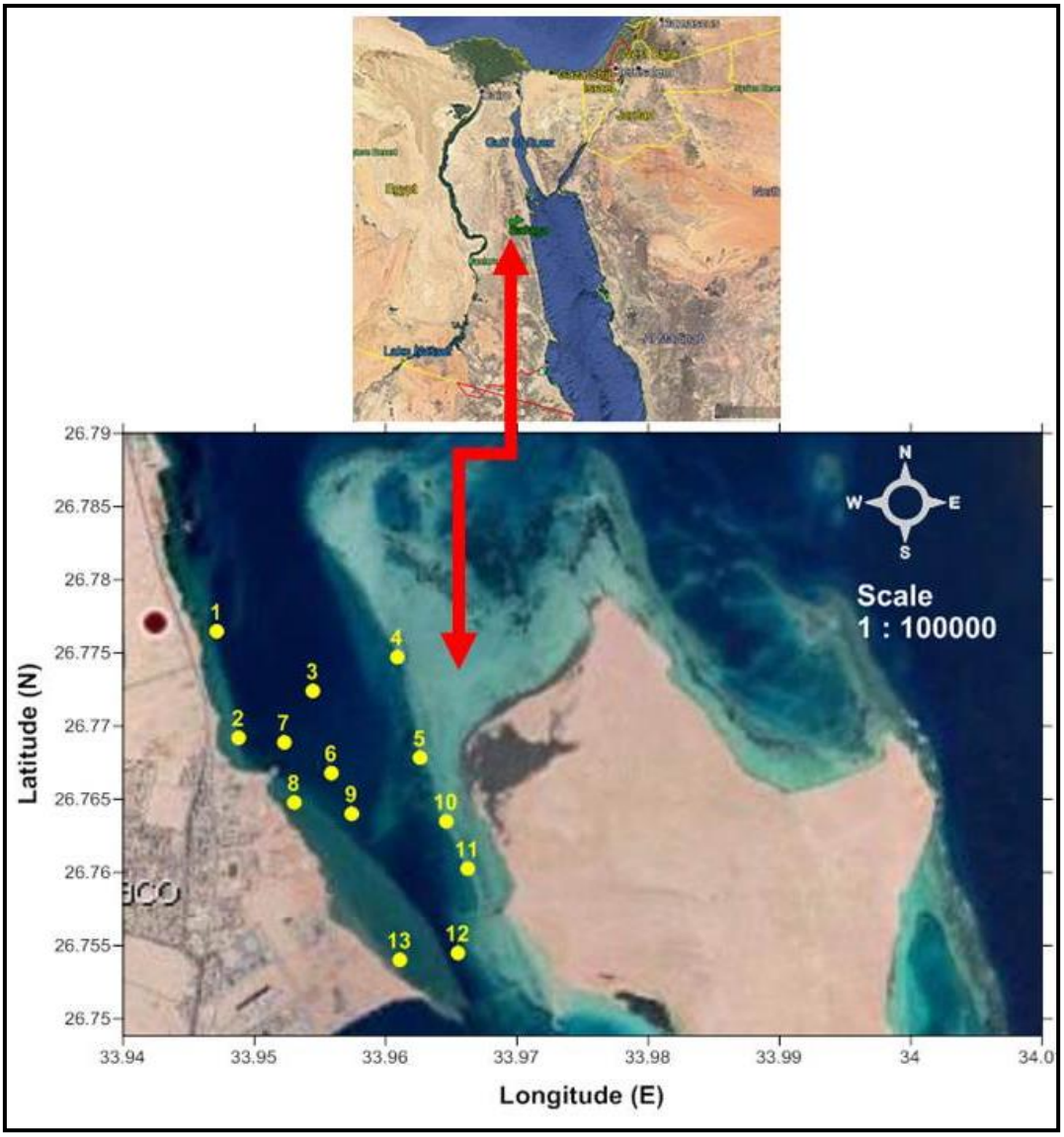

Fig. 1. Sampling sites along Safaga Bay, Red Sea, Egypt

Table 1. Oceanographic parameters of seawater of Safaga Bay, Red Sea, Egypt

Station	Latitude	Longitude	Depth (m)	Temperature (^{o}C)	Salinity (‰)	EC (mS/cm)	pH	DO (mg/L)
1	26.7736	33.9419	7	23.90	38.85	60.70	8.19	13.90
2	26.7686	33.9431	1	26.70	39.55	61.80	8.14	15.10
3	26.7706	33.9483	15	25.98	39.23	61.30	8.18	15.20
4	26.7714	33.9556	3	26.40	40.45	63.20	8.15	14.20
5	26.7672	33.9561	5	26.60	40.77	63.70	8.15	14.40
6	26.7681	33.9483	11	24.70	38.85	60.70	8.18	15.00
7	26.7672	33.9456	3	26.40	39.49	61.70	8.13	15.70
8	26.7639	33.9483	1	25.50	38.78	60.60	8.20	15.80
9	26.7647	33.9497	6	25.10	39.17	61.20	8.20	15.90
10	26.7639	33.9581	2	26.00	39.87	62.20	8.23	15.20
11	26.7608	33.96	4	25.50	39.36	61.50	8.19	13.40
12	26.7586	33.9578	22	25.20	40.00	62.50	8.16	15.30
13	26.7586	33.9517	1	26.00	39.62	61.90	8.13	15.20
Min.			1	23.90	38.78	60.60	8.13	13.40
Max.			22	26.70	40.77	63.70	8.23	15.90
Average			6.23	25.69	39.54	61.77	8.17	14.95

Grain size analysis

In the laboratory, sediment samples were air dried at room temperature. The subsamples were then sieved into a 2mm stainless steel sieve to remove pebbles or large particles. According to **Folk and Ward (1957)**, different particle sizes were analyzed. A portion of each sample was dried overnight in an oven at 50 ± 5°C to a constant weight, ground with an agate mortar and then passed through an 80-mesh sieve.

Elemental analysis

Half a gram of completely ground samples were digested in Teflon cups at 80°C with 10ml of mixed acids (HF: $HClO_4$: HNO_3) at a ratio of 1:2:3 v/v **(Oregioni & Aston, 1984)** and then diluted to 25ml with deionized water. Total metals concentrations (Al, Mn, Fe, Zn, Cu, Co, Ni, Pb, and Cd) were measured using a Flame Atomic Absorption Spectrophotometer (FAAS, Shimadzo 6800, with Autosampler 6100). Heavy metal accuracy was performed using the International Atomic Energy Agency reference material, IAEA-405. The heavy metals corresponding to the contents of the references material showed a recovery in the range from 93.5 to 102.2 %.

Treatment of data

To find out the relationships between characteristic parameters and heavy metals, statistical processing was performed on data obtained from particle size, geochemical analysis and physical parameters by Statistica version 7.0 **(Khalil *et al.*, 2016)**. Distribution maps of different variants were performed by the Golden Software Surfer Program (version 11). Principle component analysis (PCA) and cluster analysis (CA) have been widely applied; multivariate analysis reduces dimensionality to identify the sources of heavy metals in sediments **(El Zokm *et al.*, 2021; Sarikurkcu *et al.*, 2021)**. PCA, for the geochemical parameters and heavy metals of 13 sediment samples was performed by varimax rotation using SPSS Statistics 20.0 software, while correlation matrix and tree clustering analyses were estimated by Statistica 99 at $p \leq 0.05$ significance level.

RESULTS AND DISCUSSTION

Oceanographic parameters of seawater

Table (1) presents the oceanographic parameters of seawater of Safaga Bay. The depth of the studied area ranged from 1 to 22m. There is an area characterized by high depth anomalies around stations 3 and 12 (Table 1). The average seawater temperature in Safaga Bay is 25.69^{o}C. The highest and lowest temperatures (26.7 ^{o}C and 23.9 ^{o}C) are recorded at stations 2 and 1, respectively. The temperature decreases around stations 5 and 6, while around station 2, it is characterized by a positive anomaly. The data provided is consistent with the previously detected water temperature which gradually increased from the North to the South **(Madkour, 2013)**. The salinity ranges from 38.78 to 40.77 with an average of 39.54 ‰. There are positive anomalies around station 6, while negative anomalies are detected around stations 2, 5 and 12. This decrease in salinity is attributed to domestic activities, sewage and wastewater as well as coastal activities. Compared to the other stations, station 5 shows the highest salinity of 40.77‰. The electrical conductivity (EC) varies from 60.6 to 63.7 mS/cm, with an average of 61.77 mS/cm. Station 6 shows a positive EC anomaly distribution, while the area around stations 6 and 12 has an anomalous negative EC distribution. Low differences between the EC values are related to the relative similarity of the ions present **(Al-Taani *et al.*, 2020)**. The pH of seawater is weakly alkaline. The pH ranges between 8.13 and 8.23, with the highest level detected at station 10 and the lowest at stations 7 and 13. There are two distinct pH distributions. The first is a negative anomaly located near stations 5 and 7, and the second is a positive anomaly located near site 10. The dissolved oxygen (DO) changes from 13.40mg/L at station 11 to 15.9mg/L at station 9, with an average 14.95 mg/L. The DO content of seawater in Safaga is higher than that reported in the ocean seawater (3.2 - 4.8 mg/L) **(Wong & Li, 2009)**. These elevated DO levels may be attributed to the processes of oxygen production, i.e. due to the photosynthesis processes of phytoplankton and macrophytes **(Mandal *et al.*, 2012)**. The DO distribution shows negative anomalies around stations 7, 8 and 9.

Grain size distribution

Particle size analysis represents the most basic characteristics of sediment particles and affects their trapping, transport and deposition **(Krishna *et al.*, 2009)**. In the aquatic environment, the element concentration of the siliciclastic sediments mainly depends on the particle size of the sediment. Therefore, sediment grain size explores heavy metal contamination, sediment type's differentiation and biogeochemical processes **(Lim *et al.*, 2013)**. The study area received sediments from two different sources, terrestrial rock fragments from the mountains of the hinterland and biogenic carbonates from the sea (i.e., siliciclastic and carbonate sediments). The parameters used to describe grain size distribution fall into four main groups: those that measure (a) average size, (b) spread (sorting) sizes around the average, (c) symmetry or preferential spread (skewness) to one side of the average, and (d) the degree of grain concentration relative to the average (kurtosis). The studied sediments consist mainly of sand fractions with an average percentage of 93.15%. The lowest sand content (75%) occurs in the channel between northern and southern bays with an average of 6.85% (Table 2). The particle size of the sediment reveals the predominance of the sand fraction in all collected samples (Table 2). In general, particle size analysis indicates that as the distance from shore to deeper water increases, it changes from fine sand near the shore to coarse sand. The occurrence of

Table 2. Grain size analysis of sediment samples collected from Safaga Bay, Red Sea, Egypt

Station	Sand %	Mud %	Sediment type	Mean (Ø)		Sorting (Ø)		Skewness		Kurtosis	
1	100	0	Sand	2.45	Fine sand	0.53	Moderately well sorted	-0.13	Coarse skewed	1.37	Leptokurtic
2	99	1	Sand	2.87	Fine sand	0.89	Moderately sorted	-0.18	Coarse skewed	1.13	Leptokurtic
3	86	14	Sand	2.06	Fine sand	1.78	Poorly sorted	-0.11	Coarse skewed	0.8	Platykurtic
4	99	1	Sand	1.36	Medium sand	1.41	Poorly sorted	-0.06	Near symmetrical	0.85	Platykurtic
5	94	6	Sand	1.78	Medium sand	1.63	Poorly sorted	-0.02	Near symmetrical	0.83	Platykurtic
6	98	2	Sand	0.77	Coarse sand	1.45	Poorly sorted	0.25	Fine skewed	0.67	Platykurtic
7	95	5	Sand	2.6	Fine sand	0.99	Moderately sorted	-0.06	Near symmetrical	0.82	Platykurtic
8	99	1	Sand	2.16	Fine sand	1.04	Poorly sorted	-0.31	Strongly coarse skewed	1.42	Leptokurtic
9	93	7	Sand	2.36	Fine sand	1.27	Poorly sorted	-0.05	Near symmetrical	1.1	Mesokurtic
10	94	6	Sand	1.24	Medium sand	1.75	Poorly sorted	0.12	Fine skewed	0.57	Very platykurtic
11	99	1	Sand	1.2	Medium sand	1.45	Poorly sorted	0.09	Near symmetrical	0.87	Platykurtic
12	75	25	Sand	3.27	Very fine sand	1.18	Poorly sorted	-0.12	Coarse skewed	1.04	Mesokurtic
13	80	20	Sand	1.99	Medium sand	1.49	Poorly sorted	-0.32	Strongly coarse skewed	0.96	Mesokurtic
Min.	75	0		0.77		0.53		-0.32		0.57	
Max.	100	25		3.27		1.78		0.25		1.42	
Average	93.15	6.85		2.01		1.30		-0.07		0.96	

Table 3. Correlation matrix of oceanographic and sediment parameters of Safaga Bay, Red Sea, Egypt

Variable	Depth	T	pH	EC	S‰	O_2	Al	Fe	Mn	Zn	Cu	Co	Ni	Pb	Cd	Mean	Sand	Mud	Sorting	Skewness	Kurtosis
Depth	1																				
T	-0.3837	1																			
pH	0.0496	-0.4981	1																		
EC	-0.0155	**0.6485**	-0.4180	1																	
S‰	-0.0213	**0.6490**	-0.3995	**0.9996**	1																
O_2	0.0604	0.1496	-0.0069	-0.2263	-0.2224	1															
Al	-0.3254	-0.1425	-0.1547	-0.4039	-0.4089	-0.0359	1														
Fe	0.0310	0.1170	-0.2453	0.0997	0.0896	**0.6487**	-0.3102	1													
Mn	-0.1525	0.0541	-0.1213	-0.3086	-0.3129	**0.6533**	0.1925	0.5289	1												
Zn	0.0883	0.1058	-0.3027	-0.1304	-0.1360	**0.6205**	0.1063	0.4722	**0.8363**	1											
Cu	0.3693	-0.0880	-0.2550	-0.2563	-0.2597	**0.6613**	0.0249	0.4359	**0.6749**	**0.8437**	1										
Co	0.2708	0.1628	0.3004	0.4077	0.4138	-0.4922	-0.5490	-0.3634	**-0.6859**	**-0.6678**	**-0.5928**	1									
Ni	0.4725	0.2270	0.1395	0.4663	0.4702	-0.2606	**-0.7347**	-0.1501	-0.5218	-0.3840	-0.2917	**0.9153**	1								
Pb	0.0967	-0.1927	0.3980	0.1310	0.1422	**-0.6426**	-0.1312	**-0.7254**	**-0.8438**	**-0.8490**	**-0.7392**	**0.6889**	0.4819	1							
Cd	0.1968	0.1016	0.3708	0.3569	0.3646	-0.4879	**-0.6413**	-0.3326	**-0.6838**	**-0.6888**	**-0.6442**	**0.9688**	**0.8901**	**0.7280**	1						
Mean	0.2746	0.0181	-0.3521	-0.0154	-0.0246	0.4002	0.4682	0.2418	0.4909	**0.6954**	**0.6700**	**-0.5982**	-0.4604	**-0.6093**	**-0.7367**	1					
Sand	**-0.5886**	-0.0517	0.2633	-0.2425	-0.2405	-0.3440	0.4245	-0.2521	-0.2697	**-0.5698**	**-0.6126**	0.1661	-0.1752	0.2772	0.1450	-0.4097	1				
Mud	**0.5886**	0.0517	-0.2633	0.2425	0.2405	0.3440	-0.4245	0.2521	0.2697	**0.5698**	**0.6126**	-0.1661	0.1752	-0.2772	-0.1450	0.4097	**-1**	1			
Sorting	0.1080	0.3975	0.1626	0.4010	0.4102	0.0042	**-0.8342**	0.0136	-0.3036	-0.2802	-0.2812	**0.6252**	**0.7302**	0.3505	**0.7262**	**-0.5903**	-0.3054	0.3054	1		
Skewness	0.1809	-0.1681	0.3687	0.0474	0.0576	-0.3028	-0.4686	-0.1932	**-0.7054**	**-0.7056**	-0.3611	**0.6637**	**0.5615**	**0.5584**	**0.6752**	**-0.6444**	0.3123	-0.312	0.3802	1	
Kurtosis	-0.0907	-0.3796	0.0116	-0.4034	-0.4151	0.0805	**0.6876**	0.1225	0.5391	0.4141	0.1896	**-0.6153**	**-0.6967**	-0.4247	**-0.6559**	**0.5928**	0.1203	-0.12	**-0.7713**	**-0.7045**	1

Significant levels $p<0.05$ are written in bold font

fine sediments here may be due to the predominance of sediments of the terrigenous fine-size. The portion of sand in the sediments varies from 75 to 100% (Table 2). The mean sediment size ranges from 0.77 Φ (coarse sand) to 3.27 Φ (very fine sand). This indicates that mean grain size distribution mainly depends on the type of benthic facies, the distance from the shore and the depth of the water. The sorting changes from 0.53 to 1.78 Φ (i.e. from moderately well sorted to poorly sorted). Sorting differences depend on grain size (r= -0.5903, $p \leq 0.034$; Table 3); however, the coarse sediments (gravels and conglomerates), and the fine sediments (silt and clay) are more poorly sorted than the sand-sized sediments. Sand sediments are easily transported and shifted by wind and water **(Pettijohn, 1975)**. The skewness ranges from -0.32 (strongly coarse skewed) to 0.25 (fine skewed), and has a moderate correlation with mean particle size (r = -0.6444, $p \leq 0.017$) (Table 3). Negative values are due to the high energy conditions, while the positive skewness in the sheltered areas is due to the accumulation of fine materials, and/or the addition of carbonate material to the sediments (corals and seashells) **(Duane, 1964; Mohamed *et al.*, 2011; El Nemr & El-Said, 2017)**. Furthermore, kurtosis varies from very platykurtic (0.57) to leptokurtic (1.42). Kurtosis correlates somewhat positively with mean size (r = 0.5928, $p \leq 0.033$), and significantly negatively correlated with sorting (r =-0.7713, $p \leq 0.002$) and skewness (r =-0.7045, $p \leq 0.007$). The contour lines of the grain size parameters mark three distribution regions near stations 6, 10 and 12 in the northern, eastern and southern regions of the study area, respectively (Fig. 2).

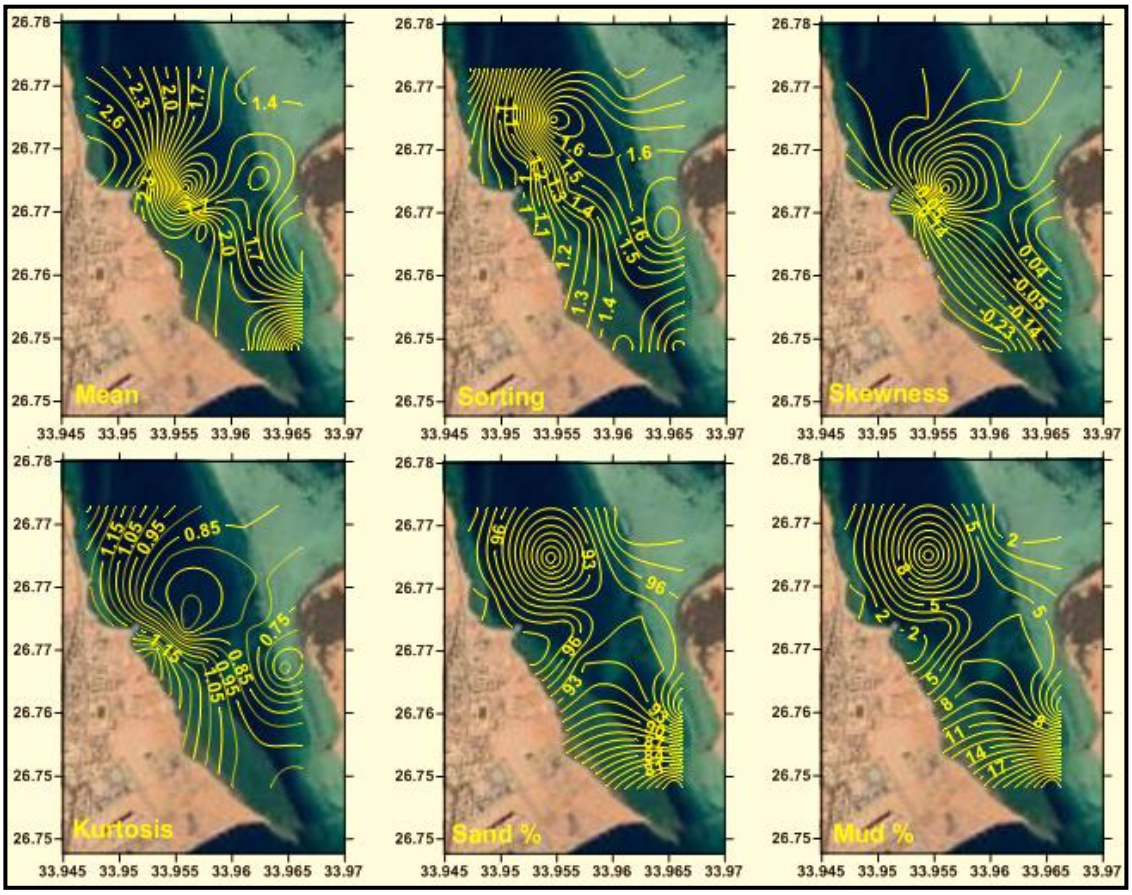

Fig. 2. Distribution pattern of grain size parameters at Safaga Bay, Red Sea, Egypt

The sorting profile and skewness gradually increase from the coast, and vice versa, for mean size and kurtosis values. The sand content increases from the South to the North, while mud content appears in the opposite direction.

Distribution of heavy metals

Table (4) and Fig. (3) illustrate the distribution of nine heavy metals (Al, Fe, Mn, Zn, Cu, Co, Ni, Pb, and Cd) in the bottom sediments. Heavy metal concentrations fluctuate across the study area with Al, being the most abundant heavy metal (average 4537.12±5025.35 mg/kg dw), followed by Fe (average 678.91±342.97 mg/kg dw), Mn (average 136.09±117.00 mg/kg dw), Zn (average 40.38±11.92 mg/kg dw), Pb (average 17.19±3.97 mg/kg dw), Ni (average 12.74±3.01 mg/kg dw), Co (average 9.24±2.19 mg/kg dw), Cu (average 2.98±1.24 mg/kg dw), and Cd (average 2.46±1.20 mg/kg dw). Their ranges are as follows: Al (564.41-14694.74 mg/kg dw), Fe (148.16-1318.27 mg/kg dw), Mn (26.86-418.17 mg/kg dw), Zn (23.09-58.26 mg/kg dw), Pb (11.47-22.52 mg/kg dw), Ni (8.34-16.72 mg/kg dw), Co (5.59-11.92 mg/kg dw), Cu (1.28-5.31 mg/kg dw), and Cd (0.99-3.94 mg/kg dw). Al registers the highest concentration at site 2; while the highest level of Fe is observed at site 9. Higher concentrations of Mn, Pb and Ni are found at stations 8, 10 and 3, respectively.

Table 4. Heavy metal concentrations (mg/kg dw) in Safaga Bay sediments, Red Sea, Egypt

Station	Al	Fe	Mn	Zn	Cu	Co	Ni	Pb	Cd
1	14599.97	148.16	53.82	31.30	2.35	7.46	8.34	22.03	1.47
2	14694.74	435.44	125.17	42.67	2.78	7.66	9.56	15.07	1.12
3	2521.38	375.07	85.13	39.07	3.06	11.42	16.72	20.55	3.60
4	2442.38	680.16	28.76	35.21	1.28	11.92	16.60	19.85	3.94
5	951.51	874.22	39.28	23.09	1.31	11.26	14.45	19.64	3.46
6	1494.75	749.37	26.86	23.60	2.53	10.61	14.60	20.39	3.41
7	6316.98	976.80	240.98	52.03	5.08	7.10	10.81	11.47	0.99
8	8338.04	973.30	418.17	52.56	3.39	7.48	9.83	12.05	1.51
9	1906.25	1318.27	164.62	46.88	3.41	7.40	10.63	13.22	1.78
10	635.09	299.41	60.15	32.00	2.33	11.23	14.78	22.52	3.74
11	1229.13	297.76	62.92	32.70	2.04	11.63	14.76	18.74	3.83
12	564.41	892.42	207.28	58.26	5.31	9.34	15.19	13.72	2.11
13	3287.98	805.51	255.97	55.61	3.84	5.59	9.34	14.22	1.09
Min.	564.41	148.16	26.86	23.09	1.28	5.59	8.34	11.47	0.99
Max.	14694.74	1318.27	418.17	58.26	5.31	11.92	16.72	22.52	3.94
Average	4537.12	678.91	136.09	40.38	2.98	9.24	12.74	17.19	2.46
SD	5025.35	342.97	117.00	11.92	1.24	2.19	3.01	3.97	1.20

Nawar and Shata (1989) reported that the increased Mn content in offshore sediments in the northern Red Sea is due to its incorporation into the calcite crystal lattice. The high concentration of Pb may be related to human activities, including mineral transport, untreated wastewater, and water flow in the mangrove area in front of location 10 **(Khaled *et al.*, 2003; Mansour *et al.*, 2013)**. The increase in Zn levels in Safaga Bay may be accompanied with the activity of shipping mineral products, especially zinc and phosphate, as well as mining activities in the Eastern Desert **(El Nemr *et al.*, 2004; El Nemr *et al.*, 2016a)**. Zinc is commonly associated with other metal such as copper, lead and cadmium **(Singh *et al.*, 2017)**. The maximum content

of Co and Cd is detected at station 4, while the highest levels of Zn and Cu are recorded at station 12. The high content of Cd in the sediments of Safaga Bay appears to be attributed to urban and industrial runoff discharge. Copper concentrations at all studied sites are below the toxicological limit (30 mg/kg dw) **(FAO, 1983)**.

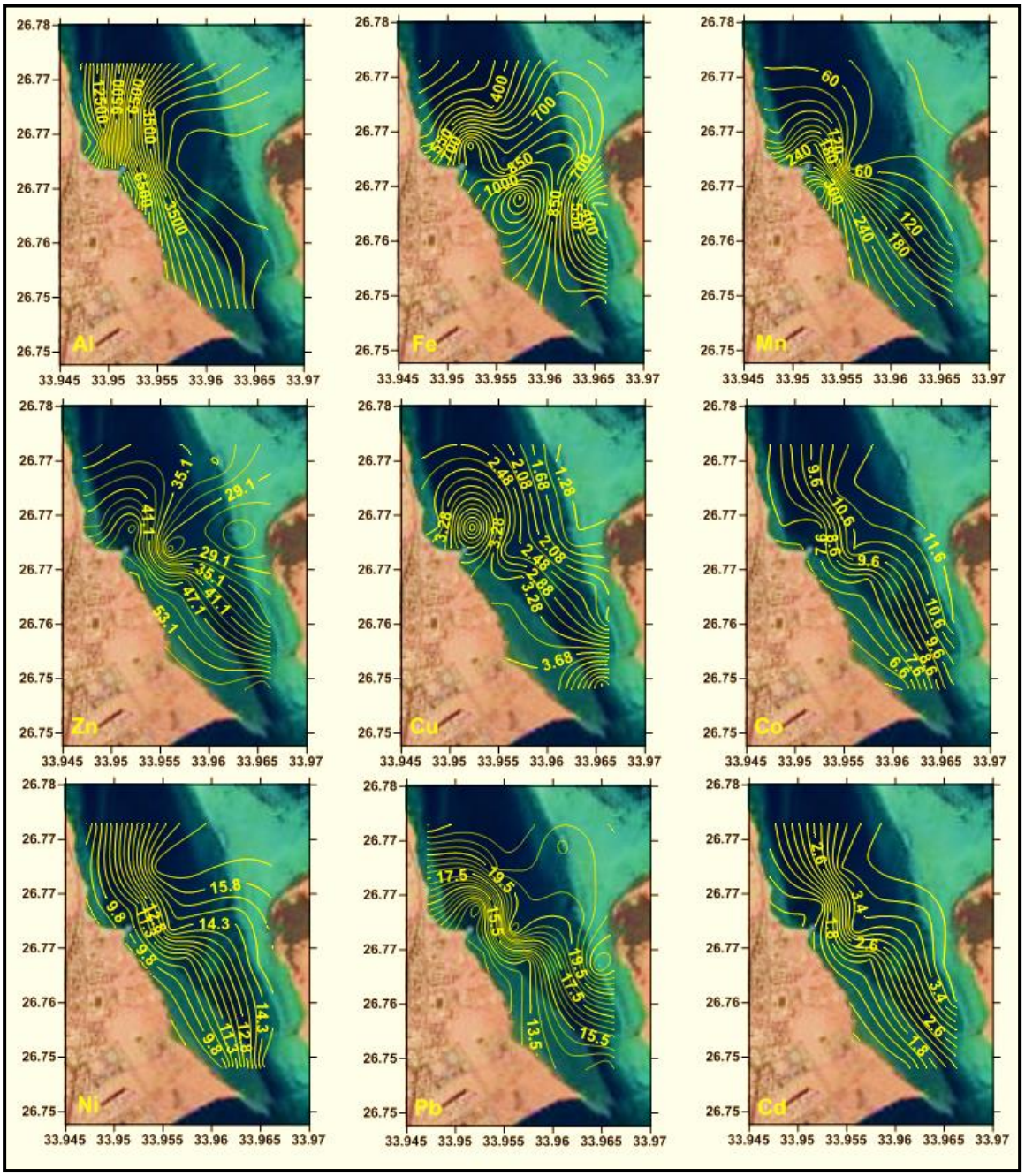

Fig. 3. Horizontal distribution of heavy metal concentrations in surface sediments of Safaga Bay, Red Sea, Egypt

The correlation matrix refers to the interaction between geochemical parameters and the distribution of heavy metals, as well as human activities such as fishing, shipping, oil exploration, aquaculture, seawater desalination, and population growth (Table 3). The high negative correlations between Zn and Co (r= -0.6678, $p \leq 0.013$), Pb (r= -0.8490), and Cd (r= -0.6888, $p \leq 0.009$) may reflect their different anthropogenic sources. Whereas, its positive relationships with Cu (r= 0.8437) and

mean grain size (r= 0.6954, $p \leq 0.008$) are likely associated with its primary contact with suspended matter before sedimentation **(Singh *et al.*, 2017)**. In addition, the correlations between Zn & sand (r=-0.5698, $p \leq 0.042$) and Zn & mud (r=0.5698, $p \leq 0.042$) confirm this observation.

Correlations of Cd, Pb, and Co with mean particle size (r = -0.7367, $p \leq 0.004$, -0.6093, $p \leq 0.027$, and -0.5982, $p \leq 0.031$, respectively) may indicate that they have similar man-made sources and contribution behaviors in the study area. Interestingly, horizontal distribution lines explore the increasing abundance of these metals towards the East coast (Fig. 2). However, these heavy metals are by-products of mining, smelting, and industrial fields and can easily be transported in the marine environment **(Singh *et al.*, 2017)**. Moreover, nickel-cadmium batteries, paints, and color production produce Cd as a by-product. Pb is found in Zn and Cu sulfide ores, and is a by-product of paints, pipes, building materials, and gasoline production. Cd and Pb can bioaccumulate and persist in the marine environment and have similar toxicity to invertebrates, fishes and plants **(Singh *et al.*, 2017)**. On the contrary, the mean particle size content is high- positively correlated with Cu (r= 0.6700, $p \leq 0.012$) and Zn (r= 0.6954, $p \leq 0.008$). Cu can destroy the root membrane cell of aquatic plants **(Singh *et al.*, 2017)**.

The correlation matrix reflects the impact of water current direction represented by sorting and skewness on the distribution of Al, Ni, Mn, Zn, Co, Pb, and Cd along the study area (Table 3). Ni can form complexes containing organic and inorganic substances **(Singh *et al.*, 2017)**. Ni can also be readily adsorbed on clay matrix in the aqueous sphere and can be precipitated in combination with iron and manganese hydroxides **(Singh *et al.*, 2017)**. It is likely that the high correlations between the dissolved oxygen content and Fe (r= 0.6487, $p \leq 0.016$) and Mn (r= 0.6533, $p \leq 0.015$) are related to the manganese-iron oxidation reduction reactions **(Kuriata-Potasznik *et al.*, 2016)**. The contents of Cd and Pb may be strongly related to the formation of hydroxides and oxides of iron and manganese in the aqueous media **(Kuriata-Potasznik *et al.*, 2016)**.

In general, since the investigated area is located in a desert belt, atmospheric dust inputs from the surrounding arid region are considered an important source of heavy metals for seawater. These properties would alter the microenvironment and thus affect the bioavailability of metals in tidal flats **(El Nemr & El-Said, 2017)**.

Table (5) shows a comparison between the average levels of heavy metals studied in the current study with those recorded in other studies over the same area and other coastal sediments along the Red Sea, the Mediterranean Sea, the Yellow Sea and the Aegean Sea. When compared to previous studies conducted on the Safaga region, the concentrations of Al, Co, and Cd were higher than those previously reported **(Salem *et al.*, 2014; Younis *et al.*, 2014; El Nemr *et al.*, 2016a, b)**, while the Zn concentration was lower than that of **El Nemr *et al.* (2016a, b)**.

A comparison between the heavy metal contents observed in the current study with those reported in the sediments collected from different parts of the world shows that the concentration of iron, manganese, zinc, copper and lead in the surface sediments of Safaga Bay is very low. The Al content in sediments from the Red Sea in Saudi Arabia **(Ruiz-Compean *et al.*, 2017)** and the Gabes Gulf, the Mediterranean Sea in Tunisia **(Naifar *et al.*, 2018)** is higher than that observed in Safga Bay. Higher concentrations of Co and Ni were detected in the surface sediments from Hurghada **(Attia & Ghrefat, 2013)**, the Egyptian Mediterranean Sea and the Suez Gulf, Red Sea, Egypt **(El-Sorogy & Attiah, 2015; El-Sikaily *et al.*, 2021)**, respectively. Compared to most of other regions, the cadmium concentration was higher.

Table 5. Comparison between heavy metal concentrations (mg/kg dw) in Safaga Bay sediments and other parts of the world

Location	Al	Fe	Mn	Zn	Cu	Co	Ni	Pb	Cd	References
Safaga Bay, Red Sea, Egypt	4537.12	678.91	136.09	40.38	2.98	9.24	12.74	17.19	2.46	Present study
Safaga, Red Sea, Egypt		5381.60	206.99	38.09	1.80	4.54	10.06	5.12	0.10	Salem *et al.*(2014)
Safaga, Red Sea, Egypt		261.03	61.84	13.49	3.46		11.51	21.25	1.65	Younis *et al.* (2014)
Safaga, Red Sea, Egypt				51.33	0.73		14.80	3.46	0.36	El Nemr *et al.* (2016a)
Safaga, Red Sea, Egypt	2202.70			60.86	0.13		8.33	1.55	0.06	El Nemr *et al.* (2016b)
Hurghada, Red Sea, Egypt			77	15.76	13.14	50.54	33.67	43.67	3.11	Attia & Ghrefat (2013)
Suez Gulf, Red Sea, Egypt		256–2225	3.1–153.4	1.5–43.3	4.2–23.04		6.9–34.2	9.9–37.1	0.7–3.3	El-Sikaily *et al.* (2021)
Red Sea, Egypt		355.44		7.77	1.26	1.66	1.74	42.38	0.14	Nour *et al.* (2018)
Red Sea, Saudi Arabia	12987.12	13531.94	213.78	26.79	9.33	6.25	14.23	5.55	0.28	Ruiz-Compean *et al.* (2017)
Red Sea, northwest Saudi Arabia	4876.56	1413.34		16.75	18.67	5.34	13.66	3.54	0.18	Kahal *et al.* (2018)
Mediterranean Sea, Egypt	240	193791.18	614.06	340.23			803.03	405.71		El-Sorogy & Attiah (2015)
Eastern Harbor, Mediterranean Sea, Egypt	3004.92	12946.92	118.76	92.17	43.15			40.57	1.11	Abdel Ghani *et al.* (2013)
Western Harbor, Mediterranean Sea, Egypt			189.54	205.72	141.27			231.37	5.05	Shreadah *et al.* (2015)
Gabes Gulf, Mediterranean Sea, Tunisia	7289	4339	73.00	104.90	37		11.08	10.71	8.14	Naifar *et al.* (2018)
Mediterranean Sea, Morocco		32620	439.74	98.72	6.92		17.49	22.47	0.12	Saddik *et al.* (2019)
South Yellow Sea			789	93.70	16.90			17.80	0.30	Yuan *et al.* (2012)
Eastern Aegean Sea			562	71	18.51			10.49	0.11	Uluturhan *et al.* (2011)
ERL				150	34.00		20.90	46.70	1.20	Long *et al.* (1995)
ERM				410	270		51.60	218	9.60	Long *et al.* (1995)
TEL (threshold effect level)				124	18.70		15.90	30.20	0.68	Macdonald *et al.* (1996)
PEL (probable effect level)				271	108		42.80	112	4.21	Macdonald *et al.* (1996)

Assessment of pollution

The following pollution indices are used to assess the quality of surface sediments in the north of Safaga Bay:

Contamination (*CF*) and degree of contamination (C_d) factors

The contamination factor *(CF)* is the ratio between the concentration of each heavy metal in the sediments and the background value (Eq.1; **Hakanson, 1980**). The degree of contamination factor (C_d) is the sum of contamination factors (Eq. 2; **Hakanson, 1980**).

$$CF = \frac{C_{Heavy\ metal}}{C_{Background}} \quad (1)$$

$$C_d = \sum_{i=1}^{n} CF \quad (2)$$

Where n is the number of contaminants present in the sediments sample.

Based on the contamination factor *(CF)*, 54 % of the examined sites are moderately contaminated with Pb ($1 \leq CF < 3$) while for Cd, 77% of the sites are very highly contaminated ($CF \geq 6$) and 23% are considerably contaminated ($3 \leq CF < 6$). For other metals, there is low contamination ($CF < 1$) (Fig. 4 and Table 6). Results of the degree of contamination factor C_d indicate that 46% of the sites show a considerable degree of contamination with metals ($16 \leq C_d < 32$), 31% have a moderate degree ($8 \leq C_d < 16$) and 23% have a low degree of contamination ($C_d < 8$) (Fig. 5a and Table 6).

Modified degree of contamination (mC_d)

It gives the average total value of a group of pollutants and is calculated by the through the following (Eq. 3; **Ibrahim *et al.*, 2019**):

$$mC_d = \frac{\sum_{i=1}^{9} CF^i}{9} \quad (3)$$

Fig. 5b shows the modified degree of contamination (mC_d) values for the sediments north of the Safaga Bay where mC_d values are shown ranging from 0.80 to 2.46. Stations 3, 4, 5, 6, 10 and 11 record high mC_d values between 2.15 and 2.46 reflecting a moderate degree of contamination. However, other stations show mC_d values less than 1.5 and reveal nil to very low degree of contamination (Table 6).

Metal pollution index (*MPI*)

The metal pollution index (*MPI*) is used to compare the total concentration of heavy metals (*Cf*) in different sampling areas **(Usero *et al.*, 1996, 1997)**. *MPI* is calculated using Eq. (4), where high *MPI* represents a high level of pollution with an element in the sample.

$$MPI = (Cf_1 \times Cf_2 \times \ldots \times Cf_n)^{1/n} \quad (4)$$

Where C_f is the concentration of heavy metal *i* in the sample, *n* is the number of studied heavy metals.

High *MPI* values are recorded for all examined sites ranging from 9.69 to 15.96 with an average of 12.36 (Fig. 5c). The highest values are observed at stations, 3, 8, 10 and 12 (14.36, 13.88, 13 and 15.96, respectively). While other stations fluctuate between 9.69 and 12.77 (Fig. 5c), indicating that the north of Safaga Bay suffers from heavy metal pollution that may be due to shipping, industrial and human activities **(Mansour *et al.*, 2013)**.

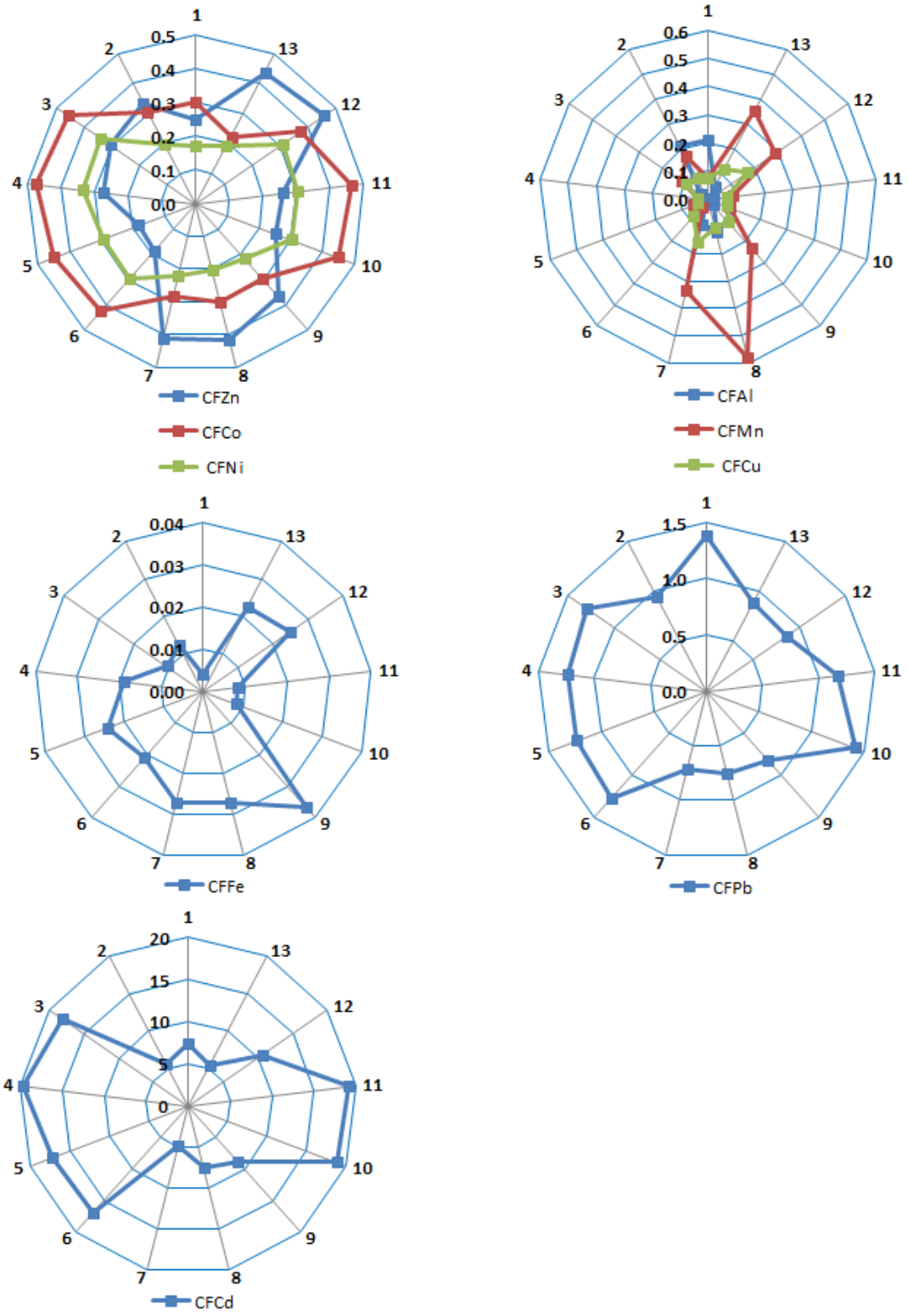

Fig. 4. Radar chart showing contamination factor (*CF*) values of heavy metals in surface sediments of Safaga Bay, Red Sea, Egypt

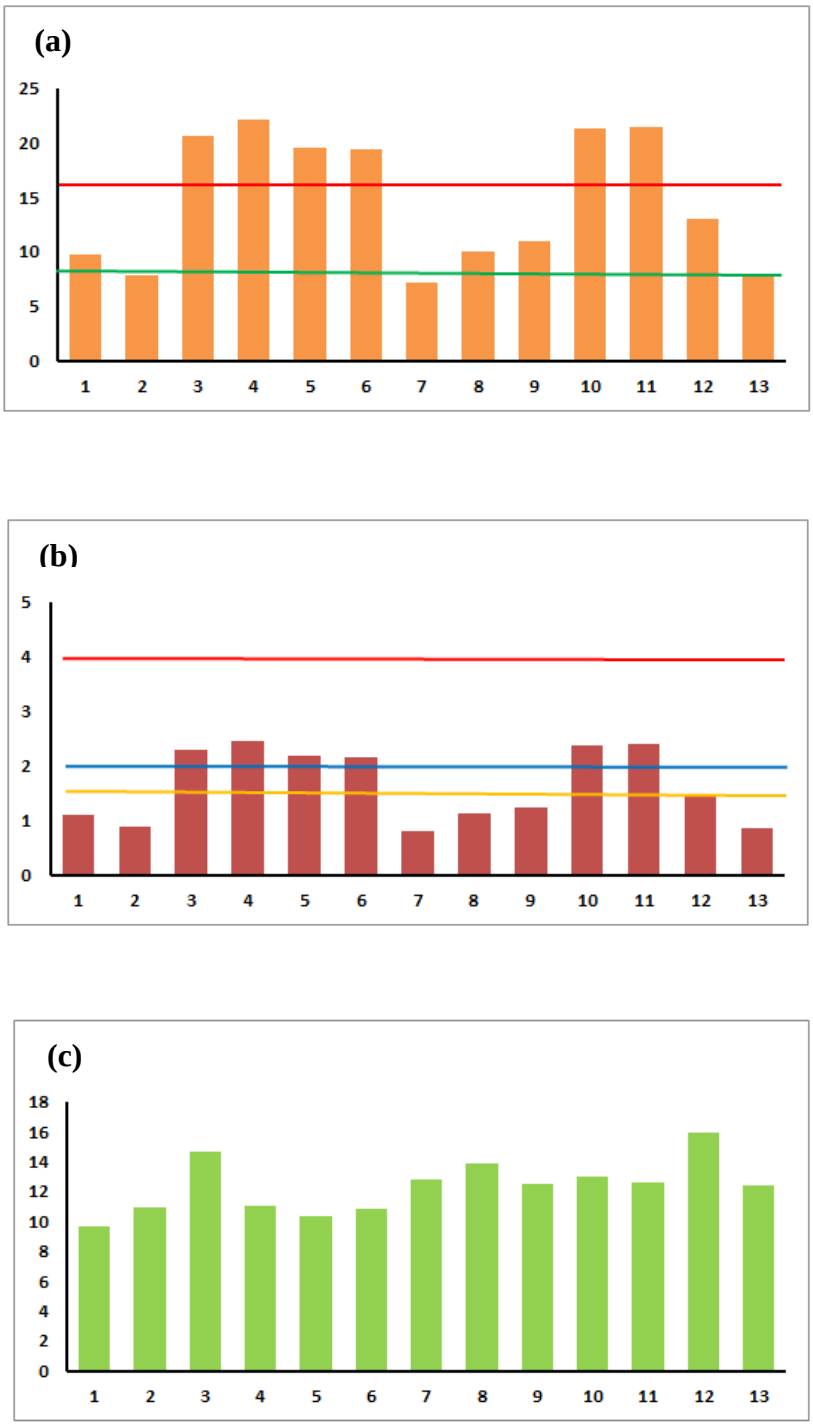

Fig. 5. (a) Degree of contamination (C_d), **(b)** modified degree of contamination (mC_d), and **(c)** metal pollution index (*MPI*) values of heavy metals in surface sediments of Safaga Bay, Red Sea, Egypt

Table 6. Contamination indices (contamination factor, degree of contamination, modified degree of contamination, and enrichment factor) used in this study and their classifications

Contamination factor (*CF*)		**Degree of contamination (C_d)**		**Modified degree of contamination (mC_d)**		**Enrichment factor (*EF*)**	
CF value	Contamination level	C_d value	Degree	mC_d value	Degree	*EF* value	Contamination level
$CF < 1$	Low	$C_d < 8$	Low	$mC_d < 1.5$	Zero to very low	$EF < 1$	No enrichment
$1 \leq CF < 3$	Moderate	$8 \leq C_d < 16$	Moderate	$1.5 < mC_d < 2$	Low	$1 < EF < 3$	Minor enrichment
$3 \leq CF < 6$	Considerable	$16 \leq C_d < 32$	Considerable	$2 < mC_d < 4$	Moderate	$3 < EF < 5$	Moderate enrichment
$CF \geq 6$	Very high	$C_d \geq 32$	Very high	$4 < mC_d < 8$	High	$5 < EF < 10$	Moderately severe enrichment
				$8 < mC_d < 16$	Very high	$10 < EF < 25$	Severe enrichment
				$16 < mC_d < 32$	Extremely high	$25 < EF < 50$	Very severe enrichment
				$mC_d \geq 32$	Ultra-high	$EF > 50$	Extremely severe enrichment (Ultr-high)

Enrichment factor (*EF*)

The enrichment factor (*EF*) is applied to assess the impact of the anthropogenic activities through the abundance of trace metals. In this study, Al is used as the reference metal for geochemical normalization to calculate *EF*, and it is estimated by Eq. (5) **(Khaled *et al.*, 2021)**:

$$EF = \left(C/Al\right)_S \Big/ \left(C/Al\right)_B \quad (5)$$

Where *(C/Al)S* is the ratio of metal to Al concentration in the sample and (*C/Al)B* is the same ratio in the crust (Earth's crust; **Martin & Meybek, 1979; Kremling & Streu, 1993; Molinari *et al.*, 1993; Liaghati *et al.*, 2003**). **Zhang & Liu (2002)** stated that elements with *EF*<2 are considered to originate from the crustal materials or natural processes, while elements with *EF*>2 are more likely to originate from anthropogenic sources. The *EF* values estimated in this study show that the northern Safaga Bay sediments are moderately severe enrichment with Mn (*EF* = 6.54), severe enrichment with Zn, Cu, Co, and Ni (*EF* = 13.07, 10.61, 17.20 and 12.31, respectively), very severe enrichment with Pb (*EF* = 47.51) and extremely severe enrichment with Cd (*EF* = 625.95). However, Fe showed *EF* values < 2 with no enrichment suggesting that it is originated from natural sources. Results also show that sediments of station 10 are highly enriched with Co, Pb and Cd while station 12 is rich in Mn, Zn, Cu and Ni (Table 6 and Fig. 6). The levels of metal enrichment in the surface sediments of Safaga Bay decreased in the following order: Cd>Pb>Co>Zn>Ni>Mn>Cu>Fe. Based on the average *EF* values of the studied

metals, it is indicated that the surface sediments of Safaga Bay are rich in metals from anthropogenic inputs.

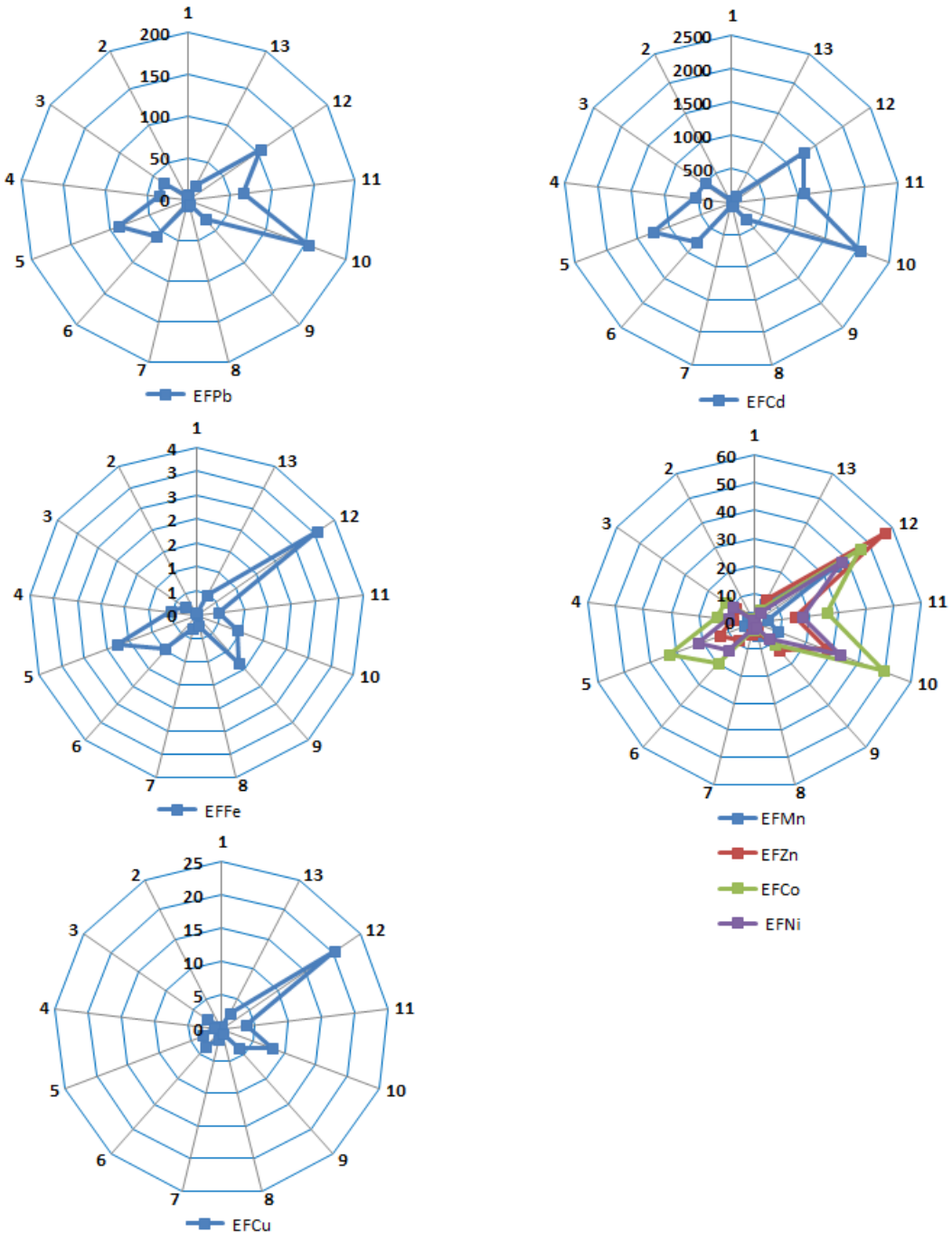

Fig. 6. Radar chart showing enrichment factor (*EF*) values of heavy metals in surface sediments of Safaga Bay, Red Sea, Egypt

Potential contamination index

The potential contamination index (*PCI*) was proposed by **Davaulter & Rognerud (2001)** to assess sediments pollution. PCI_i is determined using the following equation:

$$PCI_i = {}^{C_{imax}}/_{C_b} \quad (6)$$

Where PCI_i is the index potential contamination of metal i, $C_{i\ max}$ represents the maximum metal content i in the sediments, and C_b is the background value of the metal content of interest in the earth crust for the same metal **(Martin & Meybek, 1979; Kremling & Streu, 1993; Molinari *et al.*, 1993; Liaghati *et al.*, 2003)**. Three classes of sediment classification are distinguished (Table 7; **Davaulter & Rognerud, 2001**). Table 7 shows that the sediments samples in the study area are classified as follows: low contamination with Fe, Cu, Ni, Zn, Co, and Mn with *PCI* values of 0.04, 0.17, 0.34, 0.46, 0.48 and 0.58, respectively, moderate contamination with Pb (*PCI* = 1.41), and severe or very severe Cd contamination (*PCI* = 19.70).

Table 7. Potential risk indices in sediments of Safaga Bay, Red Sea, Egypt

Index	Value	Classification	Potential risk in Safaga Bay
PCI	< 1	Low contamination	Fe, Cu, Ni, Zn, Co, and Mn
	1< *PCI* < 3	Moderate contamination	Pb
	> 3	Severe or very severe contamination	Cd
SPI	0–2	Natural sediments	
	2–5	Low polluted sediments	46% of sediments samples
	5–10	Moderately polluted sediments	8% of sediments samples
	10–20	Highly polluted sediments	46% of sediments samples
	> 20	Dangerously polluted sediments	
E_r^i	< 40	Low ecological risk	Zn, Cu, Co, Ni, and Pb
	$40 < E_r^i \leq 80$	Modest ecological risk	
	$80 < E_r^i \leq 160$	Considerable ecological risk	8% of sediments samples for Cd
	$160 < E_r^i \leq 320$	Elevated ecological risk	46% of sediments samples for Cd
	> 320	Sever ecological risk	46% of sediments samples for Cd
RI	< 150	Low ecological risk	
	150 < *RI* < 300	Modest ecological risk	46% of sediments samples
	300 < *RI* < 600	Elevated ecological risk	46% of sediments samples
	≥ 600	Considerably high ecological risk	8% of sediments samples

Sediment pollution index

The sediment pollution index (*SPI)* is a multi-metals index for assessing sediment parameters with reference to metal content and toxicity. The *SPI* was estimated according to the following equation **(Rubio *et al.*, 2000; El Nemr & El-Said, 2017)**:

$$SPI = \sum(EF_m \times W_m)/\sum W_m \quad (7)$$

$$EF_m = {}^{C_n}/_{C_R} \quad (8)$$

Where EF_m is the ratio between the measured metal content (C_n) and the reassembled background metal content (C_R); C_R is the metal content of earth crust **(Martin & Meybek, 1979; Kremling & Streu, 1993; Molinari *et al.,* 1993; Liaghati *et al.,* 2003)**. W_m is the toxicity weight, denoted as 1, 5, 5, 5, 5 and 30 for Zn, Cu, Co, Ni, Pb and Cd, respectively **(Hakanson, 1980; Xu *et al.,* 2008)**. The *SPI* index is categorized into 5 classes as shown in Table 7. The *SPI* of the study area indicated that 46% of the sediments samples are classified as low polluted sediments, 8% of the sediments samples are moderately polluted, and 46% are classified as highly polluted sediments.

Ecological risk assessment

Sediment quality guidelines (SQGs)

These guidelines examine the enrichment of sediments with heavy metals and their harmful effects on biological life. Heavy metals levels can be assessed using US National Oceanic and Atmospheric Administration (NOAA) in terms of both Effects Range Low (*ERL*) and Effects Range Median (*ERM*) **(Long *et al.,* 1995; Christophoridis *et al.,* 2009)** and Canadian guidelines (CCME) in terms of Threshold Effect Level (*TEL*) and Probable Effect Level (*PEL*) **(CCME, 1999)**. Adverse biological effects rarely occur at levels lower than *ERL* and *TEL*. In this study, average concentrations of Zn, Cu, Ni and Pb do not exceed the NOAA and Canadian guidelines (*ERL, ERM, TEL* and *PEL*, respectively; Table 5). Thus, these heavy metals do not cause any harmful effects to the aquatic organisms in this area. However, the Cd level (2.46 mg/kg dw) exceeds *ERL* (1.2 mg/kg dw) and *TEL* (0.68 mg/kg dw) but below *ERM* and *PEL* represent a range in which toxic effects on aquatic organisms occur in sometimes.

Potential ecological risk index (*RI*)

The potential ecological risk index (*RI*) was proposed by **Hakanson (1980)**, and it has been used to assess the damage of heavy metals in sediments. *RI* is calculated using the following formulas.

$$RI = \sum E_r^i \quad (9)$$

Where E_r^i represents the potential ecological risk factor of each heavy metal. The formula of E_r^i for the single heavy metal pollution is deduced as follows:

$$E_r^i = C_f^i \times T_f^i \quad (10)$$

Where C_f^i represents the heavy metal concentration divided by the background value. T_f^i is the toxic factor of heavy metal, the values of Zn, Cu, Co, Pb, Ni and Cd are 1, 5, 5, 5, 5 and 30, respectively and *RI* is classified into four classes (Table 7; **Hakanson, 1980; Xu *et al.,* 2008**). The results of estimating potential ecological risk coefficients (E_r^i) and the integrated risk index (*RI*) for sediments samples from North Safaga region are shown in Tables 7 and 8.

Table 8. Potential ecological risk index (*RI*) of heavy metals in sediments of Safaga Bay, Red Sea, Egypt

	E_r^i						
Station	**Zn**	**Cu**	**Co**	**Ni**	**Pb**	**Cd**	***RI***
1	0.25	0.37	1.49	0.85	6.88	220.50	230.34
2	0.34	0.43	1.53	0.98	4.71	168.00	175.99
3	0.31	0.48	2.28	1.71	6.42	540.00	551.20
4	0.28	0.20	2.38	1.69	6.20	591.00	601.76
5	0.18	0.20	2.25	1.47	6.14	519.00	529.25
6	0.19	0.40	2.12	1.49	6.37	511.50	522.06
7	0.41	0.79	1.42	1.10	3.58	148.50	155.81
8	0.41	0.53	1.50	1.00	3.77	226.50	233.71
9	0.37	0.53	1.48	1.08	4.13	267.00	274.60
10	0.25	0.36	2.25	1.51	7.04	561.00	572.41
11	0.26	0.32	2.33	1.51	5.86	574.50	584.76
12	0.46	0.83	1.87	1.55	4.29	316.50	325.49
13	0.44	0.60	1.12	0.95	4.44	163.50	171.05
Average	0.32	0.46	1.85	1.30	5.37	369.81	379.11

According to the results of the potential ecological risk factor (E_r^i), the hazards of heavy metals are arranged in the following order: Cd > Pb > Co > Ni > Cu > Zn. Consequently, the estimated E_r^i for Zn, Cu, Co, Ni, and Pb is less than 40 indicating that these metals are at low ecological risk. The potential of Cd hazard is a considerable ecological risk ($80 < E_r^i \leq 160$) in about 8% of the studied sites, a high ecological risk ($160 < E_r^i \leq 320$) in about 46% of the sites, and about 46% of sediments samples have a severe ecological risk (>320). As a result, Cd may have potential hazards in sediments from the North Safaga region. Further, the *RI* values which represent the combined potential ecological risks of all studied heavy metals reflect the responsibility of Cd for heavy metal contamination in the sediments of all studied sites ranging from a moderate degree of hazard ($150 < RI < 300$; observed in 46% of sites) to high risk degrees ($300 < RI < 600$; in 46% of sites), and considerably high risk degree ($RI \geq 600$ in the remaining sites).

Statistical analysis

Hierarchical cluster analysis (HCA)

Cluster analysis (CA) was applied to the marine sediments quality data set to group the similar sampling sites identified with specific characteristics (Fig. 7). In the tree clustering, the sampling sites are grouped into three clusters at ≈ 2000 linkage distances according to the geochemical characteristics of each site. Cluster 1 identifies locations 7 and 8, cluster 2 identifies locations 3-6, and 9-13, and cluster 3 identifies locations 1 and 2. Furthermore, stations 7&8 (linkage distances ≈ 2000), and 1&2, 3&4, 5&12, and 6&11 have relatively geochemical compositions at linkage distances ≤ 1000.

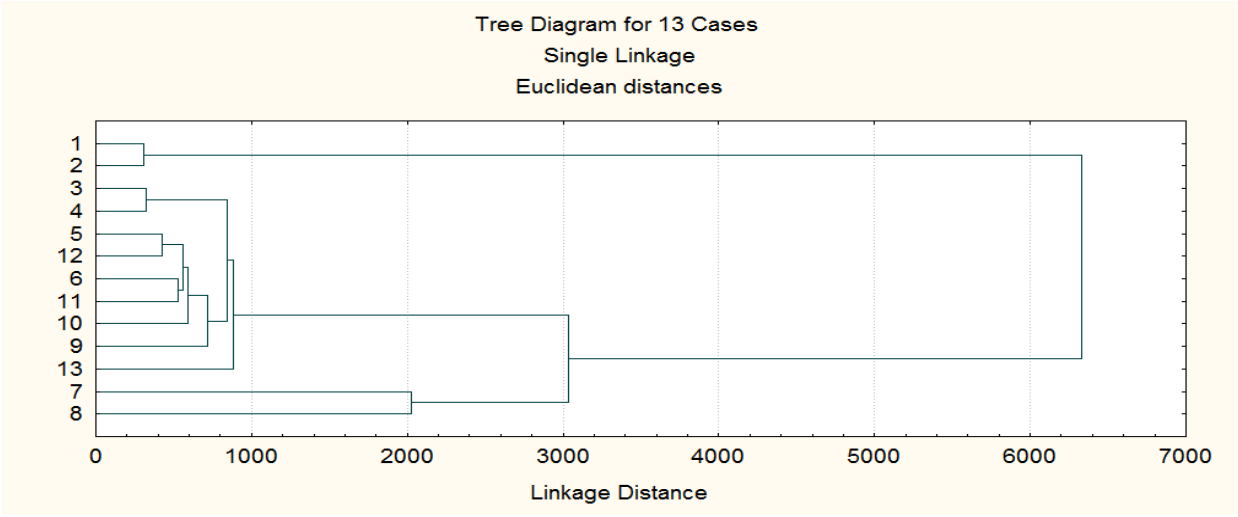

Fig. 7. Cluster analysis for the estimated parameters in sediments of different locations along Safaga Bay, Red Sea, Egypt

Principal component analysis (PCA)

PCA results show only three PCs with eigenvalues greater than or equal to 1 and a cumulative percentage of variances of 85.07 % as shown in Fig. 8 and Table 9. PC1 accounts for 38.76 of total variance and has high positive loads on Co (0.753), Ni (0.858), Cd (0.822), and sorting (0.893) and high negative loads on Al (-0.930) and kurtosis (-0.842) associated with turbulent fluctuation and sedimentation of Ni, and Cd on sediments and the stability of Al distribution and the similar anthropogenic source of Ni and Cd. PC2 contributes to 23.16 % of total variance and shows the usual inverse contribution of sand (-0.954) and mud (0.954) to the sediments texture. PC3 is articulated by Fe (0.904), Mn (0.734), and Pb (0.852) at 23.15 %, accompanied with the lithogenic origin of these heavy metals in addition to the anthropogenic origin of Mn and Pb in this area. From the statistical analysis, it appears that heavy metals may alert marine organisms and may cause additional adverse health risks to the aquatic ecosystem associated with Safaga Bay in the future.

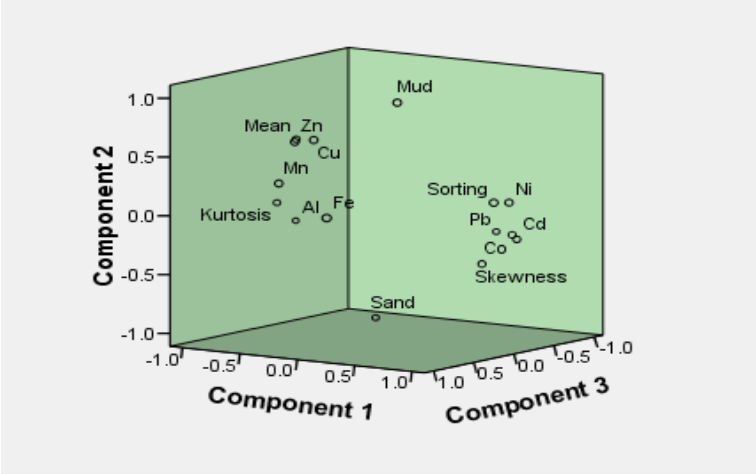

Fig. 8. Component plot in rotated space

Table 9. Principal component analysis for studied geochemical parameters and heavy metals in Safaga Bay sediments, Red Sea, Egypt

Parameter	PC1	PC2	PC3
Al	***-0.930***	-0.212	-0.198
Fe	0.112	0.075	**0.904**
Mn	-0.425	0.290	**0.734**
Zn	-0.379	0.629	0.601
Cu	-0.258	0.649	0.538
Co	**0.753**	-0.205	-0.490
Ni	**0.858**	0.108	-0.300
Pb	0.361	-0.269	**0.852**
Cd	**0.822**	-0.230	-0.449
Mean	-0.652	0.556	0.194
Sorting	**0.893**	0.145	-0.059
Skewness	0.656	- 0.428	-0.252
Kurtosis	***-0.842***	0.002	0.162
Sand	-0.191	***-0.954***	0.138
Mud	0.191	**0.954**	0.138
Variance %	38.76	23.16	23.15
CV %	38.76	61.92	85.07

Extraction Method: Principal Component Analysis, Rotation Method: Varimax with Kaiser Normalization. Rotation converged in 4 iterations

Human health risk assessment

Human health risk assessment is widely used to detect health effects that may be associated with exposure to non-carcinogenic substances **(USEPA, 2001)**. In this study, risk assessment is determined by three exposure pathways: ingestion, dermal contact, and swimming ingestion (non-carcinogenic risk; **Health Consultation 2009; Iqbal *et al.*, 2013**). These exposure pathways for adults and children were calculated using different criteria. Children and adults are separated due to their physiological and behavioral differences between them **(Wang *et al.*, 2005)**. Exposure is estimated by sediments ingestion (Exp_{Ing}) using the given equation (Eq. 11; **Yee, 2010**):

$$Exp_{Ing} = \frac{C_{Sed} \times Ing_{Sed} \times F \times RAF \times EF_{Ing} \times ED \times CF}{AT \times BW} \quad (11)$$

Where C_{Sed} = heavy metal concentration in sediments (mg/kg); Ing_{Sed} = ingestion rate (80 and 20 kg /day for child and adult, respectively); F = fraction of parameter adsorbed from site (1 for 100% of parameter); RAF = relative absorption factor for heavy metal; EF_{Ing} = exposure frequency (365 day/year); ED = exposure period (4.5 and 60 year for child and adult, respectively); CF = conversion factor (1.0×10^{-6} kg/mg); AT = average time (1642.5 and 29200 day for child and adult, respectively); BW = body weight (16.5 and 70.7 kg for child and adult, respectively).

The exposure through dermal contact (Exp_{Derm}) is evaluated as the following equation **(Qing *et al.*, 2015)**:

$$Exp_{Derm} = \frac{C_{Sed} \times EF_{Ing} \times SA \times AF \times ABS}{AT \times BW} \quad (12)$$

Where *SA* = exposed skin area 5,700 cm^2; EF_{Ing} = exposure frequency (365 day/year); *AF* = adherence factor 0.07 mg/cm^2; and *ABS* = dermal absorption factor (0.001, unit less).

Exposure is determined by ingestion of sediments while swimming (Exp_{Swim}) according to the following formula:

$$Exp_{Swim} = \frac{C_{Sed} \times IR_{Swim} \times RAF_{Sed} \times EF_{Swim}}{BW \times DPY} \quad (13)$$

Where IR_{swim} = rate of accidental ingestion of sediments while swimming (8 X 10^{-5} mg/kg); RAF_{sed} = sediments specific chemical relative absorption factor (0.58, unitless); EF_{swim} = exposure frequency (30 days/year); *DPY* = Days per year (365 days/year).

In this study, the non-carcinogenic effects of heavy metals are demonstrated using the hazard quotient (*HQ*) and hazard index (*HI*) for each exposure pathway (ingestion, dermal contact, and swimming ingestion). The hazard quotient (*HQ*) of each investigated element is assessed by using (Eq. 14; **USEPA, 2005**).

$$HQ = Exp/RfD \quad (14)$$

Where, *Exp* and *RfD* are the exposure pathway and the reference dose of each element, respectively.

The Tolerable Daily Intake (*TDI*) is used in place of the *RfD* for iron because there is no reference dose value for the dermal cutaneous dose that has been established yet **(Yee, 2010; Iqbal *et al.*, 2013)**. The *RfD* values (mg/kg day^{-1}) for Cd, Cu, Ni, Pb, Fe, Mn, Co and Zn are 0.001, 0.0371, 0.02, 0.0035, 0.7, 0.14, 0.02 and 0.3, respectively **(Yee, 2010; Kusin *et al.*, 2018)**.The *RfD* value represents the maximum acceptable dose of a metal with no serious human health effects.

The hazard index (*HI*) is the sum of the *HQ* values of all metals in the sediments and it is used to assess the generally non-carcinogenic risks posed by various metals **(Kusin *et al.*, 2018)**. *HI* values for ingestion, dermal contact and ingestion by swimming are calculated as follows:

$$HI = \sum HQ = \sum HQ_{Ing} + \sum HQ_{Derm} + \sum HQ_{Swim} \quad (15)$$

When *HQ* and *HI* are less than 1, there is no apparent risk to the population, while when *HQ* and HI are > 1 there may be concern about non-carcinogenic effects **(USEPA, 2004)**.

The current study demonstrates the health risks of studied heavy metals in sediments using exposure assessment of ingestion (Exp_{Ing}), dermal contact (Exp_{Derm}), and ingestion while swimming (Exp_{Swim}) (Table 10). Interestingly, the daily exposures (Exp_{Ing}, Exp_{Derm}, and Exp_{Swim}) to heavy metals in Safaga Bay sediments are lower than the *RfD* values of various heavy metals (Table 10).

Table 10. Exposure dose (*Exp*; mg/kg/day) through ingestion, dermal contact, and ingestion while swimming for children and adults

Station	*Exp* Fe Child	*Exp* Fe Adult	*Exp* Mn Child	*Exp* Mn Adult	*Exp* Zn Child	*Exp* Zn Adult	*Exp* Cu Child	*Exp* Cu Adult	*Exp* Co Child	*Exp* Co Adult	*Exp* Ni Child	*Exp* Ni Adult	*Exp* Pb Child	*Exp* Pb Adult	*Exp* Cd Child	*Exp* Cd Adult
1	7.18E-04	3.10E-06	2.61E-04	1.13E-06	1.52E-04	6.55E-07	1.14E-05	4.92E-08	3.62E-05	1.56E-07	4.04E-05	1.75E-07	1.07E-04	6.45E-07	7.13E-06	3.08E-08
2	2.11E-03	9.11E-06	6.06E-04	2.62E-06	2.07E-04	8.93E-07	1.35E-05	5.82E-08	3.71E-05	1.60E-07	4.64E-05	2.00E-07	7.31E-05	4.41E-07	5.43E-06	2.34E-08
3	1.82E-03	7.85E-06	4.12E-04	1.78E-06	1.89E-04	8.18E-07	1.48E-05	6.40E-08	5.54E-05	2.39E-07	8.11E-05	3.50E-07	9.96E-05	6.01E-07	1.75E-05	7.53E-08
4	3.30E-03	1.42E-05	1.39E-04	6.02E-07	1.71E-04	7.37E-07	6.21E-06	2.68E-08	5.78E-05	2.49E-07	8.05E-05	3.47E-07	9.62E-05	5.81E-07	1.91E-05	8.24E-08
5	4.24E-03	1.83E-05	1.90E-04	8.22E-07	1.12E-04	4.83E-07	6.35E-06	2.74E-08	5.46E-05	2.36E-07	7.01E-05	3.02E-07	9.52E-05	5.75E-07	1.68E-05	7.24E-08
6	3.63E-03	1.57E-05	1.30E-04	5.62E-07	1.14E-04	4.94E-07	1.23E-05	5.29E-08	5.14E-05	2.22E-07	7.08E-05	3.06E-07	9.89E-05	5.97E-07	1.65E-05	7.14E-08
7	4.74E-03	2.04E-05	1.17E-03	5.04E-06	2.52E-04	1.09E-06	2.46E-05	1.06E-07	3.44E-05	1.49E-07	5.24E-05	2.26E-07	5.56E-05	3.36E-07	4.80E-06	2.07E-08
8	4.72E-03	2.04E-05	2.03E-03	8.75E-06	2.55E-04	1.10E-06	1.64E-05	7.09E-08	3.63E-05	1.57E-07	4.77E-05	2.06E-07	5.84E-05	3.53E-07	7.32E-06	3.16E-08
9	6.39E-03	2.76E-05	7.98E-04	3.44E-06	2.27E-04	9.81E-07	1.65E-05	7.14E-08	3.59E-05	1.55E-07	5.15E-05	2.22E-07	6.41E-05	3.87E-07	8.63E-06	3.72E-08
10	1.45E-03	6.27E-06	2.91E-04	1.26E-06	1.55E-04	6.70E-07	1.13E-05	4.88E-08	5.44E-05	2.35E-07	7.17E-05	3.09E-07	1.09E-04	6.59E-07	1.81E-05	7.83E-08
11	1.44E-03	6.23E-06	3.05E-04	1.32E-06	1.59E-04	6.84E-07	9.89E-06	4.27E-08	5.64E-05	2.43E-07	7.16E-05	3.09E-07	9.09E-05	5.48E-07	1.86E-05	8.01E-08
12	4.33E-03	1.87E-05	1.00E-03	4.34E-06	2.82E-04	1.22E-06	2.57E-05	1.11E-07	4.53E-05	1.95E-07	7.36E-05	3.18E-07	6.65E-05	4.01E-07	1.02E-05	4.42E-08
13	3.91E-03	1.69E-05	1.24E-03	5.36E-06	2.70E-04	1.16E-06	1.86E-05	8.04E-08	2.71E-05	1.17E-07	4.53E-05	1.95E-07	6.89E-05	4.16E-07	5.28E-06	2.28E-08
Average (Exp_{Ing})	3.29E-03	1.42E-05	6.59E-04	2.85E-06	1.96E-04	8.45E-07	1.44E-05	4.48E-05	4.48E-05	1.93E-07	6.18E-05	2.67E-07	8.33E-05	5.03E-07	1.20E-05	5.16E-08
1	3.58E-06	7.39E-07	1.30E-06	2.68E-07	7.57E-07	1.56E-07	5.68E-08	1.17E-08	1.80E-07	3.72E-08	2.02E-07	4.16E-08	5.33E-07	1.10E-07	3.55E-08	7.33E-09
2	1.05E-05	2.17E-06	3.03E-06	6.24E-07	1.03E-06	2.13E-07	6.72E-08	1.39E-08	1.85E-07	3.82E-08	2.31E-07	4.77E-08	3.64E-07	7.52E-08	2.71E-08	5.59E-09
3	9.07E-06	1.87E-06	2.06E-06	4.25E-07	9.45E-07	1.95E-07	7.40E-08	1.53E-08	2.76E-07	5.70E-08	4.04E-07	8.34E-08	4.97E-07	1.02E-07	8.71E-08	1.80E-08
4	1.64E-05	3.39E-06	6.95E-07	1.43E-07	8.51E-07	1.76E-07	3.10E-08	6.38E-09	2.88E-07	5.95E-08	4.01E-07	8.28E-08	4.80E-07	9.90E-08	9.53E-08	1.97E-08
5	2.11E-05	4.36E-06	9.50E-07	1.96E-07	5.58E-07	1.15E-07	3.17E-08	6.53E-09	2.72E-07	5.62E-08	3.49E-07	7.21E-08	4.75E-07	9.80E-08	8.37E-08	1.73E-08
6	1.81E-05	3.74E-06	6.50E-07	1.34E-07	5.71E-07	1.18E-07	6.12E-08	1.26E-08	2.57E-07	5.29E-08	3.53E-07	7.28E-08	4.93E-07	1.02E-07	8.25E-08	1.70E-08
7	2.36E-05	4.87E-06	5.83E-06	1.20E-06	1.26E-06	2.59E-07	1.23E-07	2.53E-08	1.72E-07	3.54E-08	2.61E-07	5.39E-08	2.77E-07	5.72E-08	2.39E-08	4.94E-09
8	2.35E-05	4.85E-06	1.01E-05	2.09E-06	1.27E-06	2.62E-07	8.20E-08	1.69E-08	1.81E-07	3.73E-08	2.38E-07	4.90E-08	2.91E-07	6.01E-08	3.65E-08	7.53E-09
9	3.19E-05	6.57E-06	3.98E-06	8.21E-07	1.13E-06	2.34E-07	8.25E-08	1.70E-08	1.79E-07	3.69E-08	2.57E-07	5.30E-08	3.20E-07	6.59E-08	4.30E-08	8.88E-09
10	7.24E-06	1.49E-06	1.45E-06	3.00E-07	7.74E-07	1.60E-07	5.63E-08	1.16E-08	2.72E-07	5.60E-08	3.57E-07	7.37E-08	5.45E-07	1.12E-07	9.04E-08	1.87E-08
11	7.20E-06	1.49E-06	1.52E-06	3.14E-07	7.91E-07	1.63E-07	4.93E-08	1.02E-08	2.81E-07	5.80E-08	3.57E-07	7.36E-08	4.53E-07	9.35E-08	9.26E-08	1.91E-08
12	2.16E-05	4.45E-06	5.01E-06	1.03E-06	1.41E-06	2.91E-07	1.28E-07	2.65E-08	2.26E-07	4.66E-08	3.67E-07	7.58E-08	3.32E-07	6.84E-08	5.10E-08	1.05E-08
13	1.95E-05	4.02E-06	6.19E-06	1.28E-06	1.34E-06	2.77E-07	9.29E-08	1.92E-08	1.35E-07	2.79E-08	2.26E-07	4.66E-08	3.44E-07	7.09E-08	2.64E-08	5.44E-09
Average (Exp_{Derm})	1.64E-05	3.39E-06	3.29E-06	6.79E-07	9.77E-07	2.01E-07	7.20E-08	1.49E-08	2.23E-07	4.61E-08	3.08E-07	6.35E-08	4.16E-07	8.57E-08	5.96E-08	1.23E-08
1	3.42E-05	7.99E-06	1.24E-05	2.90E-06	7.23E-06	1.69E-06	5.43E-07	1.27E-07	1.72E-06	4.02E-07	1.93E-06	4.50E-07	5.09E-06	1.19E-06	3.40E-07	7.93E-08
2	1.01E-04	2.35E-05	2.89E-05	6.75E-06	9.86E-06	2.30E-06	6.42E-07	1.50E-07	1.77E-06	4.13E-07	2.21E-06	5.16E-07	3.48E-06	8.13E-07	2.59E-07	6.04E-08
3	8.67E-05	2.02E-05	1.97E-05	4.59E-06	9.03E-06	2.11E-06	7.07E-07	1.65E-07	2.64E-06	6.16E-07	3.86E-06	9.02E-07	4.75E-06	1.11E-06	8.32E-07	1.94E-07
4	1.57E-04	3.67E-05	6.65E-06	1.55E-06	8.14E-06	1.90E-06	2.96E-07	6.90E-08	2.75E-06	6.43E-07	3.84E-06	8.95E-07	4.59E-06	1.07E-06	9.11E-07	2.13E-07
5	2.02E-04	4.72E-05	9.08E-06	2.12E-06	5.34E-06	1.25E-06	3.03E-07	7.07E-08	2.60E-06	6.07E-07	3.34E-06	7.79E-07	4.54E-06	1.06E-06	8.00E-07	1.87E-07
6	1.73E-04	4.04E-05	6.21E-06	1.45E-06	5.45E-06	1.27E-06	5.85E-07	1.36E-07	2.45E-06	5.72E-07	3.37E-06	7.88E-07	4.71E-06	1.10E-06	7.88E-07	1.84E-07
7	2.26E-04	5.27E-05	5.57E-05	1.30E-05	1.20E-05	2.81E-06	1.17E-06	2.74E-07	1.64E-06	3.83E-07	2.50E-06	5.83E-07	2.65E-06	6.19E-07	2.29E-07	5.34E-08
8	2.25E-04	5.25E-05	9.66E-05	2.26E-05	1.21E-05	2.84E-06	7.83E-07	1.83E-07	1.73E-06	4.03E-07	2.27E-06	5.30E-07	2.78E-06	6.50E-07	3.49E-07	8.15E-08
9	3.05E-04	7.11E-05	3.80E-05	8.88E-06	1.08E-05	2.53E-06	7.88E-07	1.84E-07	1.71E-06	3.99E-07	2.46E-06	5.73E-07	3.06E-06	7.13E-07	4.11E-07	9.60E-08
10	6.92E-05	1.62E-05	1.39E-05	3.24E-06	7.40E-06	1.73E-06	5.38E-07	1.26E-07	2.60E-06	6.06E-07	3.42E-06	7.97E-07	5.20E-06	1.21E-06	8.64E-07	2.02E-07
11	6.88E-05	1.61E-05	1.45E-05	3.39E-06	7.56E-06	1.76E-06	4.71E-07	1.10E-07	2.69E-06	6.27E-07	3.41E-06	7.96E-07	4.33E-06	1.01E-06	8.85E-07	2.07E-07
12	2.06E-04	4.81E-05	4.79E-05	1.12E-05	1.35E-05	3.14E-06	1.23E-06	2.86E-07	2.16E-06	5.04E-07	3.51E-06	8.19E-07	3.17E-06	7.40E-07	4.88E-07	1.14E-07
13	1.86E-04	4.35E-05	5.92E-05	1.38E-05	1.29E-05	3.00E-06	8.87E-07	2.07E-07	1.29E-06	3.02E-07	2.16E-06	5.04E-07	3.29E-06	7.67E-07	2.52E-07	5.88E-08
Average (Exp_{Swim})	1.57E-04	3.66E-05	3.14E-05	7.34E-06	9.33E-06	2.18E-06	6.88E-07	1.61E-07	2.14E-06	5.15E-07	2.94E-06	6.87E-07	3.97E-06	9.27E-07	5.70E-07	1.33E-07

Also, the hazard quotients (HQ_{Ing}, HQ_{Derm}, and HQ_{Swim}) and the estimated *HI* values (Table 11) are below the safety limit (<1). This indicates that the examined heavy metals will not cause any harmful non-carcinogenic health risks to human health. The highest (*HI*) value for children is recorded for Pb while for adults, it is recorded for Mn. The *HI* values decrease in the following order: Pb > Cd > Fe > Mn > Ni > Co > Zn > Cu for children and Mn > Pb > Cd > Fe > Ni > Co > Zn > Cu for adults (Table 11). The results indicate that the non-carcinogenic risks of exposure to heavy metals for children are higher due to different physiological characteristics properties compared to adults **(Wang *et al.*, 2005)**.

Table 11. Average hazard quotient (*HQ*) and cumulative hazard index (*HI*) for non-carcinogenic risk

Metal	HQ_{Ing}		HQ_{Derm}		HQ_{Swim}		*HI*	
	Child	Adult	Child	Adult	Child	Adult	Child	Adult
Fe	4.70E-03	2.00E-05	2.35E-05	4.84E-06	2.24E-04	5.23E-05	1.15E-02	1.81E-04
Mn	4.71E-03	4.71E-03	2.35E-05	4.85E-06	2.25E-04	5.24E-05	4.96E-03	4.77E-03
Zn	6.53E-04	2.82E-06	3.26E-06	6.71E-07	3.11E-05	7.26E-06	6.87E-04	1.07E-05
Cu	3.61E-04	1.56E-06	1.80E-06	3.71E-07	1.72E-05	4.02E-06	3.71E-04	5.94E-06
Co	2.24E-03	9.67E-06	1.12E-05	2.30E-06	1.07E-04	2.50E-05	2.36E-03	3.69E-05
Ni	3.09E-03	1.33E-05	1.54E-05	3.25E-06	1.47E-04	3.43E-05	3.25E-03	5.09E-05
Pb	2.08E-02	1.26E-04	1.04E-04	2.14E-05	9.93E-04	2.32E-04	2.19E-02	3.79E-04
Cd	1.20E-02	5.16E-05	5.96E-05	1.23E-05	5.70E-04	1.33E-04	1.26E-02	2.06E-04

CONCLUSION

The potential impact of several heavy metals (Al, Fe, Mn, Zn, Pb, Ni, Co, Cu, and Cd) was evaluated in the northern Safaga Bay sediments along the Red Sea, Egypt. Oceanographic parameters were determined to characterize seawater and sediments. Dissolved oxygen changed from 13.40 mg/L to 15.90 mg/L with an average of 14.95 mg/L and was higher than that reported for the ocean seawater. The sediments consisted mainly of a sandy texture with an average content of 93.15% and the mean grain size values were directly dependent on the type of sediments texture, distance from shore and water depth. The concentrations of Mn, Zn, Cu and Pb were very low compared to the concentrations of most of the world's coasts. The enrichment factor (*EF*) values indicated that it was highly severe enriched with Cd, very severe enriched with Pb, severe enriched with Co, Zn, Ni and Cu but moderately severe enriched with Mn revealing human sources of these heavy metals. A high contamination factor (*CF*) was obtained for Cd (12.32) indicating very high contamination. High values of the metal pollution index (*MPI*) were observed for all stations examined, showing that the north of Safaga Bay suffers from heavy metal pollution that may be attributed to shipping, industrial and human activities. *SQGs* demonstrated that the adverse biological effects of the heavy metals were sometimes associated with Cd, and rarely with Zn, Cu, Ni and Pb. Diverse sources human activities are located throughout the study area such as fishing, ship maintenance yards, ports, minerals transportation, untreated waste, the mining activities, tourism activities, urban and industrial runoff discharge as well as the atmospheric dust input from the surrounding areas. Non-carcinogenic risks were determined for heavy metals assessment by three pathways of exposure: ingestion, skin contact and

swimming ingestion of children and adults. Interestingly, the present results did not reflect any risks to human health from heavy metals, as, the values of Exp_{Ing}, Exp_{Derm}, and Exp_{Swim}) for the northern Safaga Bay sediments were lower than the *RfD* values for various heavy metals. Also, the HQ_{Ing}, HQ_{Derm}, and HQ_{Swim} values for the heavy metals examined and the estimated *HI* values for children and adults were below the safety limit (<1). Therefore, it is necessary to monitor heavy metals in this area to evaluate their risks and their gradual deterioration in the long term.

Conflict of interest

Authors declare that there is no conflict of interest.

REFERENCES

Abd El Wahab, M.; Melegy, A. and Helal, S. (2011). Distribution and enrichment of heavy metals in recent sediments of Safaga Bay, Egypt. Mar. Georesources Geotechnol., 29(4): 364–375. https://doi.org/ 10.1080/1064119X.2011.586014

Abdel Ghani, S.; El Zokm, G.; Shobier, A.; Othman, T. and Shreadah, M. (2013). Metal pollution in surface sediments of Abu-Qir Bay and Eastern Harbour of Alexandria, Egypt. Egypt. J. Aquat. Res., 39: 1–12. https://doi.org/10.1016/j.ejar.2013.03.001

Al-Taani, A.A.; Rashdan, M.; Nazzal, Y.; Howari, F.; Iqbal, J.; Al-Rawabdeh, A.; Al Bsoul, A. and Khashashneh, S. (2020). Evaluation of the Gulf of Aqaba Coastal water, Jordan. Water, 12(8): 2125. https://doi.org/10.3390/w12082125

Attia, O.E.A. and Ghrefat, H. (2013). Assessing heavy metal pollution in the recent bottom sediments of Mabahiss Bay, North Hurghada, Red Sea, Egypt. Environ. Monit. Assess., 185(12): 9925–9934. https://doi.org/10.1007/s10661-013-3302-4

Ayadi, N.; Alloul, F. and Bouzid, J. (2015). Assessment of contaminated sediment by phosphate fertilizer industrial waste using pollution indices and statistical techniques in the Gulf of Gabes (Tunisia). Arab. J. Geosci., 8: 1755–1767. https://doi.org/10.1007/s12517-014-1291-4

Badawy, W.M.; El-Taher, A.; Frontasyeva, M.V.; Madkour, H.A. and Khater, A.E.M. (2018). Assessment of anthropogenic and geogenic impacts on marine sediments along the coastal areas of Egyptian Red Sea. Appl. Radiat. Isot., 140: 314–326. https://doi.org/10.1016/j.apradiso.2018.07.034

Billah, M.M.; Abu Hena, M.K.; Idris, M.H.B. and Ismail, J.B. (2017). Mangrove macroalgae as biomonitors of heavy metal contamination in a tropical estuary, Malaysia. Water Air Soil Pollut., 228: 347. https://doi.org/10.1007/s11270-017-3500-8

Carvalho, S.; Kürten, B.; Krokos, G.; Hoteit, I. and Ellis, J. (2019). The Red Sea. In: "World Seas: An Environmental Evaluation". Sheppard, C. (Ed.). The Indian Ocean to the Pacific, Academic Press, London, pp. 49–74.

CCME (1999) Canadian sediment quality guidelines for the protection of aquatic life, Winnipeg, Canada: Canadian Council of Ministers of the Environment

Christophoridis, C.; Dedepsidis, D. and Fytianos, K. (2009). Occurrence and distribution of selected heavy metals in the surface sediments of Thermaikos Gulf, N. Greece. Assessment using pollution indicators. J. Hazard. Mater., 168(2-3): 1082–1091. https://doi.org/10.1016/j.jhazmat.2009.02.154

Davaulter, V. and Rognerud, S. (2001). Heavy metal pollution in sediments of the Pasvik River drainage. Chemosphere, 42(1): 9–18. https://doi.org/10.1016/S0045-6535(00)00094-1

Duane, D.B. (1964). Significance of skewness in recent sediments, Western Pamlico Sound, North California. J. Sed. Petrol., 34: 864–874

El Nemr, A.; El Sikaily, A.; Khaled, A.; Said, T.O. and Abd-Alla, A.M.A. (2004). Determination of hydrocarbons in mussels from the Egyptian Red Sea Coast. Environ. Monit. Assess., 96: 251–261. https://doi.org/10.1023/B:EMAS.0000031731.88863.25

El Nemr, A. and El-Said, G.F. (2017). Assessment and ecological risk of heavy metals in sediment and molluscs from the Mediterranean Coast. Water Environ. Res., 89(3): 195–210. https://doi.org/10.2175/106143016X14798353399458

El Nemr, A.; El-Said, G.F.; Khaled, A. and Ragab, S. (2016a). Distribution and ecological risk assessment of some heavy metals in coastal surface sediments along the Red Sea, Egypt. Int. J. Sediment Res., 31(2): 164–172. https://doi.org/10.1016/j.ijsrc.2014.10.001

El Nemr, A.; El-Said, G.F.; Ragab, S.; Khaled, A. and El-Sikaily, A. (2016b). The distribution, contamination and risk assessment of heavy metals in sediment and shellfish from the Red Sea coast, Egypt. Chemosphere, 165: 369–380. https://doi.org/10.1016/j.chemosphere.2016.09.048

El-Metwally, M.E.A.; Madkour, A.G.; Fouad, R.R.; Mohamedein, L.I.; Nour Eldine, H.A.; Dar, M.A. and El-Moselhy, K.M. (2017). Assessment the leachable heavy metals and ecological risk in the surface sediments inside the Red Sea ports of Egypt. Int. J. Mar. Sci., 7(23): 214–228. https://doi.org/10.5376/ijms.2017.07.0023

El-Sikaily, A.; Ghoniem, D.G.; Emam, M.A. and El-Nahrery, E.M.A. (2021). Biological indicators for environmental quality monitoring of marine sediment in Suez Gulf, Egypt. Egypt. J. Aquat. Res., 47: 125–132. https://doi.org/10.1016/j.ejar.2021.04.003

El-Sikaily, A.; Khaled, A. and El Nemr, A. (2005). Leachable and total heavy metals in muddy and sandy sediments collected from Suez Gulf. Egypt. J. Aquat. Res., 31: 99–119.

El-Sorogy, A.S. and Attiah, A. (2015). Assessment of metal contamination in coastal sediments, seawaters and bivalves of the Mediterranean Sea coast, Egypt. Mar. Pollut. Bull., 101(2): 867–871. https://doi.org/10.1016/j.marpolbul.2015.11.017

El-Taher, A., Zakaly, H.M.H. and Elsaman, R. (2018). Environmental implications and spatial distribution of natural radionuclides and heavy metals in sediments from four harbors in the Egyptian Red Sea coast. Appl. Radiat. Isot., 131: 13–22. https://doi.org/10.1016/j.apradiso.2017.09.024

El Zokm, G.M.; El-Said, G.F. and El Sayed, A.A.M. (2021). Combining multivariate statistical analysis to shed light on distribution and interaction of halogens in two economic ports along Red Sea Coast in Egypt. Oceanologia, 64(1): 103-116. https://doi.org/10.1016/j.oceano.2021.09.007

FAO (1983). Compilation of legal limits for hazardous substances in fish and fishery products. FAO Fish. Circ No 464: 5–100.

Fiedler, S.; Siebe, C.; Herre, A.; Roth, B.; Cram, S. and Stahr, K. (2009). Contribution of oil industry activities to environmental loads of heavy metals in the Tabasco Lowlands, Mexico. Water Air Soil Pollut., 197: 35–47. https://doi.org/10.1007/s11270-008-9789-6

Folk, R.L. and Ward, W.C. (1957). Brazos River bar: a study in the significance of grain size. J. Sediment. Petrol., 27(1): 3–26.

Gladstone, W.; Curley, B. and Shokri, M.R. (2013). Environmental impacts of tourism in the Gulf and the Red Sea. Mar. Pollut. Bull., 72(3): 375–388. https://doi.org/10.1016/j.marpolbul.2012.09.017

Hakanson, L. (1980). An ecological risk index for aquatic pollution control, a sedimentological approach. Water Res., 14(8):975–1001. https://doi.org/10.1016/0043-1354(80)90143-8

Health Consultation (2009) Metals in clam and sediment samples from Selawik, Alaska, March 25, 2009, US Department of Health and Human Services, Public Health Service, Agency for Toxic Substances and Disease Registry, Division of Health Assessment and Consultation, Atlanta, GA, USA

Ibrahim, M.I.A.; Mohamed, L.A.; Mahmoud, M.G.; Shaban, Kh.S.; Fahmy, M.A. and Ebeid, M.H. (2019). Potential ecological hazards assessment and prediction of sediment heavy metals pollution along the Gulf of Suez, Egypt. Egypt. J. Aquat. Res., 45(4): 329-335. https://doi.org/10.1016/j.ejar.2019.12.003

Iqbal, J.; Tirmizi, S.A. and Shah, M.H. (2013). Statistical apportionment and risk assessment of selected metals in sediments from Rawal Lake (Pakistan). Environ. Monit. Assess., 185: 729–743. https://doi.org/10.1007/s10661-012-2588-y

Islam, M.S.; Ahmed, M.K.; Raknuzzaman, M.; Al-Mamun, M.H. and Islam, M.K. (2015). Heavy metal pollution in surface water and sediment: a preliminary assessment of an urban river in a developing country. Ecol. Indic., 48: 282–291. https://doi.org/10.1016/j.ecolind.2014.08.016

Kahal, A.Y.; El-Sorogy, A.S.; Alfaifi, H.J.; Almadani, S. and Ghrefat, H.A. (2018). Spatial distribution and ecological risk assessment of the coastal surface sediments from the Red Sea, northwest Saudi Arabia. Mar. Pollut. Bull., 137: 198–208. https://doi.org/10.1016/j.marpolbul.2018.09.053

Khaled, A.; Ahdy, H.H.H.; Hamed, E.S.A.E.; Ahmed, H.O.; Abdel Razek, F.A. and Fahmy, M.A. (2021). Spatial distribution and potential risk assessment of heavy metals in sediment along Alexandria Coast, Mediterranean Sea, Egypt. Egypt. J. Aquat. Res., 47: 37–43. https://doi.org/10.1016/j.ejar.2020.08.006

Khaled, A.; El Nemr, A. and El Sikaily, A. (2003). Contamination of coral reef by heavy metals along the Egyptian Red Sea coast. Bull. Environ. Contam. Toxicol., 71: 577–584. https://doi.org/10.1007/s00128-003-8751-y

Khalil, M.Kh.; Draz, S.E.O; El Zokm, G.M. and El-Said, G.F. (2016). Apportionment of geochemistry, texture's properties, and risk assessment of some elements in surface sediments from Bardawil Lagoon, Egypt. Human Ecolog. Risk. Assess., 22(3): 775–791. https://doi.org/10.1080/10807039.2015.1107714

Kremling, K. and Streu, P. (1993). Saharan dust influence trace element fluxes in deep North Atlantic subtropical waters. Deep Sea Res. Part I Oceanogr. Res. Pap., 40(6): 1155–1168. https://doi.org/10.1016/0967-0637(93)90131-L

Krishna, A.K.; Satyanarayanan, M. and Govil, P.K. (2009). Assessment of heavy metal pollution in water using multivariate statistical techniques in an industrial area: A case study from Patancheru, Medak District, Andhra Pradesh, India. J. Hazard. Mater., 167(1–3): 366–373. https://doi.org/10.1016/j.jhazmat.2008.12.131

Kuriata-Potasznik, A.; Szymczyk, S.; Skwierawski, A.; Glińska-Lewczuk, K. and Cymes, I. (2016). Heavy metal contamination in the surface layer of bottom sediments in a flow-through lake: A case study of Lake Symsar in Northern Poland. Water, 8(8): 358. https://doi.org/10.3390/w8080358

Kusin, F.M.; Azani, N.N.M.; Hasan, S.N.M. and Sulong, N.A. (2018). Distribution of heavy metals and metalloid in surface sediments of heavily-mined area for bauxite ore in Pengerang, Malaysia and associated risk assessment. CATENA, 165: 454–464. https://doi.org/10.1016/j.catena.2018.02.029

Liaghati, T.; Preda, M. and Cox, M. (2003). Heavy metal distribution and controlling factors within coastal plain sediments, Bells Creek catchments, southeast Queensland, Australia. Environ. Int. 29(7): 935–948. https://doi.org/10.1016/S0160-4120(03)00060-6

Lim, D.; Choi, J.Y.; Shin, H.H.; Rho, K.C. and Jung, H.S. (2013). Multielement geochemistry of offshore sediments in the southeastern Yellow Sea and implications for sediment origin and dispersal. Quat. Int., 298: 196–206. https://doi.org/10.1016/j.quaint.2013.01.004

Long, E.R.; MacDonald, D.D.; Smith, S.L. and Calder, F.D. (1995). Incidence of adverse biological effects within ranges of chemical concentrations in marine and estuarine sediments. Environ. Manage., 19: 81–97. https://doi.org/10.1007/BF02472006

Maanan, M.; Saddik, M.; Maanan, M.; Chaibi, M.; Assobhei, O. and Zourarah, B. (2014). Environmental and ecological risk assessment of heavy metals in sediments of Nador lagoon, Morocco. Ecol. Indic., 48: 616–626. https://doi.org/10.1016/j.ecolind.2014.09.034

Macdonald, D.D.; Carr, R.S.; Calder, F.D.; Long, E.R. and Ingersoll, C.G. (1996). Development and evaluation of sediment quality guidelines for Florida coastal waters. Ecotoxicology, 5: 253–278. https://doi.org/10.1007/BF00118995

Madkour, H.A. (2013) Impacts of human activities and natural inputs on heavy metal contents of many coral reef environments along the Egyptian Red Sea coast. Arab. J. Geosci., 6: 1739–1752. https://doi.org/10.1007/s12517-011-0482-5

Mandal, S.; Debnath, M.; Ray, S.; Ghosh, P.B.; Roy, M. and Ray, S. (2012). Dynamic modelling of dissolved oxygen in the creeks of Sagar Island, Hooghly-Matla estuarine system, West Bengal, India. Appl. Math. Mod., 36(12): 5952–5963. https://doi.org/10.1016/J.APM.2011.10.013

Mansour, A.M.; Askalany, M.S.; Madkour, H.A.; Bakheit, B. and Assran, B.B. (2013). Assessment and comparison of heavy-metal concentrations in marine sediments in view of tourism activities in Hurghada area, northern Red Sea, Egypt. Egypt. J. Aquat. Res., 39(2): 91–103. https://doi.org/10.1016/j.ejar.2013.07.004

Martin, J.M. and Meybeck, M. (1979). Elemental mass-balance of material carried by major world rivers. Mar. Chem., 7(3): 173–206. https://doi.org/10.1016/0304-4203(79)90039-2

Mohamed, M.A.E., Madkour, H.A. and El-Saman, M.I. (2011). Impact of anthropogenic activities and natural inputs on oceanographic characteristics of water and geochemistry of surface sediments in different sites along the Egyptian Red Sea coast. Afr. J. Environ. Sci. Technol., 5(7): 494–511.

Molinari, E.; Guerzon, S. and Rampazzo, G. (1993). Contribution of Saharan dust to the central Mediterranean Basin. Geol. Soc. Am. Spec. Pap., 284: 303–312. https://doi.org/10.1130/SPE284-p303

Naifar, I.; Pereira, F.; Zmemla, R.; Bouaziz, M.; Elleuch, B. and Garcia, D. (2018). Spatial distribution and contamination assessment of heavy metals in marine sediments of the southern coast of Sfax, Gabes Gulf, Tunisia. Mar. Pollut. Bull., 131: 53–62. https://doi.org/10.1016/j.marpolbul.2018.03.048

Nawar, A.H. and Shata, M.A. (1989). Geochemistry of carbonate fraction in Mersa El-Aat near seashore sediments, Northern Red Sea, Egypt. Bull. Fac. Sci. Zagazig Univ., 11: 225–236.

Nour, H.E.; El-Sorogy, A.S.; Abdel Wahab, M.; Almadani, S.; Alfaifi, H. and Youssef, M. (2018). Assessment of sediment quality using different pollution indicators and statistical analyses, Hurghada area, Red Sea coast, Egypt. Mar. Pollut. Bull., 133: 808–813. https://doi.org/10.1016/j.marpolbul.2018.06.046

Nour, H.E.; Helal, S.A. and Abdel Wahab, M. (2022). Contamination and health risk assessment of heavy metals in beach sediments of Red Sea and Gulf of Aqaba, Egypt. Mar. Pollut. Bull., 177: 113517. https://doi.org/10.1016/j.marpolbul.2022.113517

Oregioni, B. and Aston, S.R. (1984). The determination of selected trace metals in marine sediments by flameless/flame atomic absorption spectrophotometry, IAEA Manaco laboratory, Internal Report (Cited from Reference Method in pollution studies N., 38, UNEP. 1986)

Pan, K.; Lee, O.O.; Qian, P.Y. and Wang, W.X. (2011). Sponges and sediments as monitoring tools of metal contamination in the eastern coast of the Red Sea, Saudi Arabia. Mar. Pollut. Bull., 62(5): 1140–1146. https://doi.org/10.1016/j.marpolbul.2011.02.043

Pettijohn, F.J. (1975). Sedimentary Rocks, third ed. Harper and Row, New York, NY, USA

Qing, X.; Yutong, Z. and Shenggao, L. (2015). Assessment of heavy metal pollution and human health risk in urban soils of steel industrial city (Anshan), Liaoning, Northeast China. Ecotoxicol. Environ. Saf., 120(2015): 377–385. https://doi.org/10.1016/j.ecoenv.2015.06.019

Rubio, B.; Nombela, M.A. and Vilas, F. (2000). Geochemistry of major and trace elements in sediments of the Ria de Vigo (NW Spain): An assessment of metal pollution. Mar. Pollut. Bull., 40: 968–80. https://doi.org/10.1016/S0025-326X(00)00039-4

Ruiz-Compean, P.; Ellis, J.; Cúrdia, J.; Payumo, R.; Langner, U.; Jones, B. and Carvalho, S. (2017) Baseline evaluation of sediment contamination in the shallow coastal areas of Saudi Arabian Red Sea. Mar. Pollut. Bull., 123(1–2): 205–218. https://doi.org/10.1016/j.marpolbul.2017.08.059

Saddik, M.; Fadili, A. and Makan, A. (2019). Assessment of heavy metal contamination in surface sediments along the Mediterranean coast of Morocco. Environ. Monit. Assess., 191: 197. https://doi.org/10.1007/s10661-019-7332-4

Salem, D.M.S.A.; Khaled, A.; El Nemr, A. and El-Sikaily, A. (2014). Comprehensive risk assessment of heavy metals in surface sediments along the Egyptian Red Sea coast. Egypt. J. Aquat. Res., 40(4): 349–362. https://doi.org/10.1016/j.ejar.2014.11.004

Sarikurkcu, C.; Akata, I. and Tepe, B. (2021). Metal concentration and health risk assessment of eight Russula mushrooms collected from Kizilcahamam-Ankara,

Turkey. Environ. Sci. Pollut. Res., 28: 15743–15754. https://doi.org/10.1007/s11356-020-11833-6

Shreadah, M.A.; Shobier, A.H.; Abdel Ghani, S.A.; El Zokm, G.M. and Said, T.O. (2015). Major ions anomalies and contamination status by trace metals in sediments from two hot spots along the Mediterranean coast of Egypt. Environ. Monit. Assess., 187: 280. https://doi.org/10.1007/s10661-015-4420-y

Singh, H.; Pandey, R.; Singh, S.K. and Shukla, D.N. (2017). Assessment of heavy metal contamination in the sediment of the River Ghaghara, a major tributary of the River Ganga in Northern India. Appl. Water. Sci., 7: 4133–4149. https://doi.org/10.1007/s13201-017-0572-y

Soliman, N.; Thabet, W.M.; El-Sadaawy, M.M. and Morsy, F.A. M. (2022). Contamination status and potential risk of metals in marine sediments of Shalateen coast, the Red Sea, Soil Sediment Contam.: An International Journal, 31(1): 40–56. https://doi.org/10.1080/15320383.2021.1903832

Ugochukwu, C.N.C. and Leton, T.G. (2004). Effluent monitoring of an oil servicing company and its impact on the environment. Afr. J. Environ. Assess. Manag., 8: 27–30.

Uluturhan, E.; Kontas, A. and Can, E. (2011). Sediment concentrations of heavy metals in the Homa Lagoon (Eastern Aegean Sea): assessment of contamination and ecological risks. Mar. Pollut. Bull., 62(9): 1989-1997. https://doi.org/10.1016/j.marpolbul.2011.06.019

USEPA (U.S. Environmental Protection Agency) (2004). Risk Assessment Guidance for Superfund Volume I: Human Health Evaluation Manual (Part E, Supplemental Guidance for Dermal Risk Assessment); USEPA: Washington, DC, USA

USEPA (U.S. Environmental Protection Agency) Region 6 (2005). USAEPA, Multimedia Planning and Permitting Division, Office of Solid Waste, Center for Combustion Science and Engineering

USEPA (U.S. Environmental Protection Agency) (2001). Toxics Release Inventory: Public Data Release Report. Available online: www.epa.gov/tri/tridata/tri01 (Accessed on 24 February 2015)

Usero, J.; González-Regalado, E. and Gracia, I. (1996). Trace metals in the bivalve mollusc *Chamelea gallina* from the Atlantic coast of southern Spain. Mar. Pollut. Bull., 32(3): 305–310. https://doi.org/10.1016/0025-326X(95)00209-6

Usero, J.; González-Regalado, E. and Gracia, I. (1997). Trace metals in bivalve molluscs *Ruditapes decussates* and *Ruditapes philippinarum* from the Atlantic coast of Southern Spain. Environ. Int., 23(3): 291–298. https://doi.org/10.1016/S0160-4120(97)00030-5

Vasiliu, D.; Bucse, A.; Lupascu, N.; Ispas, B.; Gheablau, C. and Stanescu, I. (2020). Assessment of the metal pollution in surface sediments of coastal Tasaul Lake (Romania). Environ. Monit. Assess., 192: 749. https://doi.org/10.1007/s10661-020-08698-0

Wang, H.; Wang, J.; Liu, R.; Yu, W. and Shen, Z. (2015a). Spatial variation, environmental risk and biological hazard assessment of heavy metals in surface sediments of the Yangtze River estuary. Mar. Pollut. Bull., 93(1–2): 250–258. https://doi.org/10.1016/j.marpolbul.2015.01.026

Wang, L.; Xu, Y.; Wen, H.; Tang, M.; Zhao, G.; Han, Q.; Xu, X.; Ying, M.; Hu, Z. and Xu, H. (2020). Contamination evaluation and source identification of heavy metals in sediments near outlet of Shekou industrial district of Shenzhen

City. Environ. Monit. Assess., 192: 772. https://doi.org/10.1007/s10661-020-08755-8

Wang, X.; Sato, T. and Xing, B. (2005). Health risks of heavy metals to the general public in Tianjin, China via consumption of vegetables and fish. Sci. Total. Environ., 350: 28–37. https://doi.org/10.1016/j.scitotenv.2004.09.044

Wang, Y.; Yang, L.; Kong, L.; Liu, E.; Wang, L. and Zhu, J. (2015b). Spatial distribution, ecological risk assessment and source identification for heavy metals in surface sediments from Dongping Lake, Shandong, East China. Catena, 125: 200–205. https://doi.org/10.1016/j.catena.2014.10.023

Wong, G.T.F. and Li, K.Y. (2009). Winkler's method overestimates dissolved oxygen in seawater: Iodate interference and its oceanographic implications. Mar. Chem., 115(1–2): 86–91. https://doi.org/10.1016/j.marchem.2009.06.008

Xu, Z.Q.; Ni, S.J.; Tuo, X.G. and Zang, C.J. (2008). Calculation of heavy metals toxicity coefficient in the evaluation of potential ecological risk index. Environ. Sci. Tech., 31: 112–115.

Yee, D. (2010). Technical Data Report, Human Health Risk Assessment, Enbridge Northern Gateway Project, AMEC Earth & Environmental, Calgary, AL, Canada

Younis, A.M., Ismail, I.S.; Mohamedein, L.I. and Ahmed, S.F. (2014). Spatial variation and environmental risk assessment of heavy metal in the surficial sediments along the Egyptian Red Sea coast. CATRINA, 10(1): 19–26. https://doi.org/10.12816/0010694

Yuan, H.; Song, J.; Li, X.; Li, N. and Duan, L. (2012). Distribution and contamination of heavy metals in surface sediments of the South Yellow Sea. Mar. Pollut. Bull., 64(10): 2151–2159. https://doi.org/10.1016/j.marpolbul.2012.07.040

Zhang, J. and Liu, C.L. (2002). Riverine composition and estuarine geochemistry of particulate metals in China—weathering features, anthropogenic impact and chemical fluxes. Estuar. Coast. Shelf Sci., 54(6): 1051–1070. https://doi.org/10.1006/ecss.2001.0879